International Journal of Control
Publication details, including instructions for authors and subscription information:
http://www.tandfonline.com/loi/tcon20

Minimum modelling retrospective cost adaptive control of uncertain Hammerstein systems using auxiliary nonlinearities

Jin Yan[a] & Dennis S. Bernstein[a]
[a] Department of Aerospace Engineering, University of Michigan, Ann Arbor, MI, USA
Accepted author version posted online: 01 Oct 2013.Published online: 15 Oct 2013.

To cite this article: Jin Yan & Dennis S. Bernstein (2014) Minimum modelling retrospective cost adaptive control of uncertain Hammerstein systems using auxiliary nonlinearities, International Journal of Control, 87:3, 483-505, DOI: 10.1080/00207179.2013.842264

To link to this article: http://dx.doi.org/10.1080/00207179.2013.842264

International Journal of Control, 2014
Vol. 87, No. 3, 483–505, http://dx.doi.org/10.1080/00207179.2013.842264

Minimum modelling retrospective cost adaptive control of uncertain Hammerstein systems using auxiliary nonlinearities

Jin Yan and Dennis S. Bernstein*

Department of Aerospace Engineering, University of Michigan, Ann Arbor, MI, USA

(*Received 20 January 2013; accepted 4 September 2013*)

We augment retrospective cost adaptive control (RCAC) with auxiliary nonlinearities to address a command-following problem for uncertain Hammerstein systems with possibly non-monotonic input nonlinearities. We assume that only one Markov parameter of the linear plant is known and that the input nonlinearity is uncertain. Auxiliary nonlinearities are used within RCAC to create a globally non-decreasing composite input nonlinearity. The required modelling information for the input nonlinearity includes the intervals of monotonicity as well as values of the nonlinearity that determine overlapping segments of the range of the nonlinearity within each interval of monotonicity.

Keywords: adaptive control; Hammerstein system; uncertain input nonlinearity; command-following problem

1. Introduction

A *Hammerstein system* consists of linear dynamics preceded by an input nonlinearity as considered in Haddad and Chellaboina (2001), Zaccarian and Teel (2011), and Giri and Bai (2010). This nonlinearity may represent the properties of an actuator, such as saturation to reflect magnitude restrictions on the control input, dead zone to represent actuator stiction, or a signum function to represent on–off operation. The ability to invert the input nonlinearity is often precluded in practice by the fact that the nonlinearity may be neither one-to-one nor onto, and it may also be uncertain.

If the input nonlinearity is uncertain, then adaptive control may be useful for learning the characteristics of the nonlinearity online and compensating for the distortion that it introduces. Adaptive inversion control of Hammerstein systems with uncertain input nonlinearities and linear dynamics is considered in Kung and Womack (1984a, 1984b) and Tao and Kokotović (1996).

In the present paper, we apply retrospective cost adaptive control (RCAC) along with auxiliary nonlinearities that account for the presence of the input nonlinearity. RCAC is applicable to linear plants that are possibly Multiple-input multiple-output (MIMO), non-minimum phase (NMP), and unstable as shown in Venugopal and Bernstein (2000), Hoagg, Santillo, and Bernstein (2008), Santillo and Bernstein (2010), Hoagg and Bernstein (2010, 2011, 2012), and D'Amato, Sumer, and Bernstein (2011a, 2011b). RCAC relies on the knowledge of Markov parameters and, for NMP open-loop unstable plants, estimates of the NMP zeros. This information can be obtained from either analytical modelling or system identification, see Fledderjohn, Holzel, Palanthandalam-Madapusi, Fuentes, and Bernstein (2010). As shown in D'Amato et al. (2011a), the Markov parameters provide an approach to matching the phase of the plant at the frequencies present in the command and disturbances. Alternative phase-matching techniques are given in Sumer, Holzel, D'Amato, and Bernstein (2012).

To address input nonlinearities, we make no attempt to identify or invert the input nonlinearity. The purpose of the auxiliary nonlinearities is to ensure that RCAC is applied to a Hammerstein system with a globally non-decreasing composite input nonlinearity. In particular, if the input nonlinearity is not non-decreasing, then an auxiliary blocking nonlinearity $\mathcal{N}_b$, an auxiliary sorting nonlinearity $\mathcal{N}_s$, and an auxiliary reflection nonlinearity $\mathcal{N}_r$ are used to create a composite nonlinearity $\mathcal{N} \circ \mathcal{N}_r \circ \mathcal{N}_s \circ \mathcal{N}_b$ that is non-decreasing, thus preserving the signs of the Markov parameters of the linearised system. An additional auxiliary saturation nonlinearity $\mathcal{N}_{\mathrm{sat}}$, which is used to tune the transient response of the closed-loop system, may depend on estimates of the range of the input nonlinearity and the gain of the linear dynamics.

In Kung and Womack (1984a, 1984b), Tao and Kokotović (1996), the input nonlinearities are assumed to be piecewise linear. The present paper does not impose this restriction. A preliminary version of some of the results in this paper is given in Yan, D'Amato, Sumer, Hoagg, and Bernstein (2012) and Yan and Bernstein (2013).

The contents of the paper are as follows. In Section 2, we describe the Hammerstein command-following problem. In Section 3, we summarise the RCAC algorithm. In Section 4,

*Corresponding author. Email: dsbaero@umich.edu

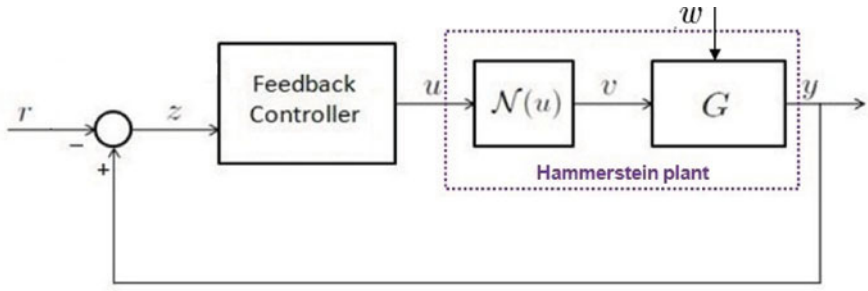

Figure 1. Adaptive command-following problem for a Hammerstein plant with input nonlinearity $\mathcal{N}$. We assume that measurements of $z(k)$ are available for feedback; however, measurements of $v(k) = \mathcal{N}(u(k))$ and $w(k)$ are not available.

we apply an extension of RCAC using auxiliary nonlinearities to the Hammerstein command-following problem with non-monotonic input nonlinearities. Next, we present examples to illustrate the construction of the auxiliary nonlinearities. Numerical simulation results are presented in Sections 5–7. In Section 5, we consider the case where the input nonlinearities are odd. In Section 6, we propose two approaches for the case where input nonlinearities are even. In Section 7, we present examples for the case where the input nonlinearities are neither odd nor even. Conclusions are given in Section 8.

2. Hammerstein command-following problem

Consider the Single-input single-output (SISO) discrete-time Hammerstein system:

$$x(k+1) = Ax(k) + B\mathcal{N}(u(k)) + D_1 w(k), \tag{1}$$

$$y(k) = Cx(k), \tag{2}$$

where $x(k) \in \mathbb{R}^n$, $u(k)$, $y(k) \in \mathbb{R}$, $w(k) \in \mathbb{R}^d$, $\mathcal{N} : \mathbb{R} \to \mathbb{R}$, and $k \geq 0$. To avoid unnecessary complications, we assume that $\mathcal{N}$ is piecewise right continuous. We consider the Hammerstein command-following problem with the performance variable:

$$z(k) = y(k) - r(k), \tag{3}$$

where $z(k) \in \mathbb{R}$ is the performance variable and $r(k) \in \mathbb{R}$ is the command. The goal is to develop an adaptive output feedback controller that minimises the command-following error z using minimal modelling information about the dynamics, disturbance w, and input nonlinearity $\mathcal{N}$. We assume that measurements of $z(k)$ are available for feedback; however, measurements of $v(k) = \mathcal{N}(u(k))$ are not available. A block diagram for Equations (1)–(3) is shown in Figure 1.

3. Controller construction

To formulate an adaptive control algorithm for Equations (1)–(3), we use a strictly proper time-series controller with auxiliary nonlinearities $\mathcal{N}_{\text{sat}}$, $\mathcal{N}_b$, $\mathcal{N}_s$, and $\mathcal{N}_r$ to account for the presence of the input nonlinearity $\mathcal{N}$ in Figure 2. The construction of $\mathcal{N}_{\text{sat}}, \mathcal{N}_b, \mathcal{N}_s$, and $\mathcal{N}_r$ is described in Section 4. The RCAC controller of order n_c is given by

$$u_c(k) = \sum_{i=1}^{n_c} M_i(k) u_c(k-i) + \sum_{i=1}^{n_c} N_i(k) z(k-i), \tag{4}$$

where for all $i = 1, \ldots, n_c$, $M_i(k) \in \mathbb{R}$, and $N_i(k) \in \mathbb{R}$. The control (4) can be expressed as

$$u_c(k) = \theta(k)\phi(k-1),$$

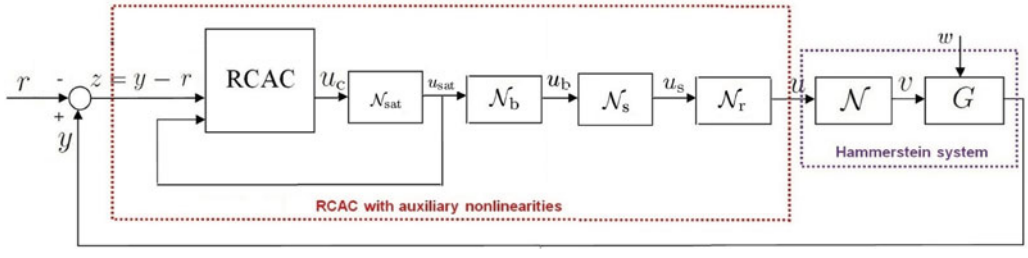

Figure 2. Hammerstein command-following problem with the RCAC adaptive controller and auxiliary nonlinearities $\mathcal{N}_{\text{sat}}$, $\mathcal{N}_b$, $\mathcal{N}_s$, and $\mathcal{N}_r$.

where

$$\theta(k) \triangleq [\, M_1(k) \cdots M_{n_c}(k)\ N_1(k) \cdots N_{n_c}(k)\,] \in \mathbb{R}^{1\times 2n_c}$$

is the controller gain matrix, and the regressor vector $\phi(k)$ is given by

$$\phi(k-1) \triangleq [u_c(k-1)\cdots u_c(k-n_c) \times z(k-1)\cdots z(k-n_c)]^T \in \mathbb{R}^{2n_c\times 1}.$$

The transfer function matrix $G_{c,k}(\mathbf{q})$ from z to u_c at time step k can be represented by

$$G_{c,k}(\mathbf{q}) \triangleq \frac{N_1(k)\mathbf{q}^{n_c-1} + N_2(k)\mathbf{q}^{n_c-2} + \cdots + N_{n_c}(k)}{\mathbf{q}^{n_c} - \left(M_1(k)\mathbf{q}^{n_c-1} + \cdots + M_{n_c-1}(k)\mathbf{q} + M_{n_c}(k)\right)},$$

where the forward shift operator $\mathbf{q}$ accounts for both the free and forced response of the system.

Next, for $i \geq 1$, define the Markov parameter:

$$H_i \triangleq CA^{i-1}B.$$

For example, $H_1 = CB$ and $H_2 = CAB$. Let ℓ be a positive integer. Then, for all $k \geq \ell$, Equation (1) can be written as

$$x(k) = A^\ell x(k-\ell) + \sum_{i=1}^{\ell} A^{i-1}B[\mathcal{N}\circ\mathcal{N}_b\circ\mathcal{N}_s\circ\mathcal{N}_r\circ\mathcal{N}_{\text{sat}}(u_c(k-i))] + \sum_{i=1}^{\ell} A^{i-1}D_1 w(k-i), \tag{5}$$

and thus

$$z(k) = CA^\ell x(k-\ell) + \sum_{i=1}^{\ell} CA^{i-1}D_1 w(k-i) - r(k) + \bar{H}\bar{U}(k-1), \tag{6}$$

where

$$\bar{H} \triangleq [\, H_1 \cdots H_\ell\,] \in \mathbb{R}^{1\times\ell}$$

and

$$\bar{U}(k-1) \triangleq \begin{bmatrix} \mathcal{N}\circ\mathcal{N}_b\circ\mathcal{N}_s\circ\mathcal{N}_r\circ\mathcal{N}_{\text{sat}}(u_c(k-1)) \\ \vdots \\ \mathcal{N}\circ\mathcal{N}_b\circ\mathcal{N}_s\circ\mathcal{N}_r\circ\mathcal{N}_{\text{sat}}(u_c(k-\ell)) \end{bmatrix}.$$

Next, we rearrange the columns of $\bar{H}$ and the components of $\bar{U}(k-1)$ and partition the resulting matrix and vector so that

$$\bar{H}\bar{U}(k-1) = \mathcal{H}'U'(k-1) + \mathcal{H}U(k-1), \tag{7}$$

where $\mathcal{H}' \in \mathbb{R}^{1\times(\ell-l_U)}$, $\mathcal{H} \in \mathbb{R}^{1\times l_U}$, $U'(k-1) \in \mathbb{R}^{\ell-l_U}$, and $U(k-1) \in \mathbb{R}^{l_U}$. Then, we can rewrite Equation (6) as

$$z(k) = \mathcal{S}(k) + \mathcal{H}U(k-1), \tag{8}$$

where

$$\mathcal{S}(k) \triangleq CA^\ell x(k-\ell) + \sum_{i=1}^{\ell} CA^{i-1}D_1 w(k-i) - r(k) + \mathcal{H}'U'(k-1). \tag{9}$$

Next, for $j = 1, \ldots, s$, we rewrite Equation (8) with a delay of k_j time steps, where $0 \leq k_1 \leq k_2 \leq \cdots \leq k_s$, in the form

$$z_j(k-k_j) = \mathcal{S}_j(k-k_j) + \mathcal{H}_j U_j(k-k_j-1), \tag{10}$$

where Equation (9) becomes

$$\mathcal{S}_j(k-k_j) \triangleq CA^\ell x(k-k_j-\ell) + \sum_{i=1}^{\ell} CA^{i-1}D_1 w(k-k_j-i) - r(k-k_j) + \mathcal{H}'_j U'_j(k-k_j-1)$$

and Equation (7) becomes

$$\bar{H}\bar{U}(k-k_j-1) = \mathcal{H}'_j U'_j(k-k_j-1) + \mathcal{H}_j U_j(k-k_j-1),$$

where $\mathcal{H}'_j \in \mathbb{R}^{1\times(\ell-l_{U_j})}$, $\mathcal{H}_j \in \mathbb{R}^{1\times l_{U_j}}$, $U'_j(k-k_j-1) \in \mathbb{R}^{\ell-l_{U_j}}$, and $U_j(k-k_j-1) \in \mathbb{R}^{l_{U_j}}$. Now, by stacking $z(k-k_1), \ldots, z(k-k_s)$, we define the *extended performance:*

$$Z(k) \triangleq \begin{bmatrix} z_1(k-k_1) \\ \vdots \\ z_s(k-k_s) \end{bmatrix} \in \mathbb{R}^s. \tag{11}$$

Therefore,

$$Z(k) = \tilde{\mathcal{S}}(k) + \tilde{\mathcal{H}}\tilde{U}(k-1), \tag{12}$$

where

$$\tilde{\mathcal{S}}(k) \triangleq \begin{bmatrix} \mathcal{S}_1(k-k_1) \\ \vdots \\ \mathcal{S}_s(k-k_s) \end{bmatrix} \in \mathbb{R}^s.$$

$\tilde{U}(k-1)$ has the form,

$$\tilde{U}(k-1) \triangleq \begin{bmatrix} \mathcal{N} \circ \mathcal{N}_b \circ \mathcal{N}_s \circ \mathcal{N}_r \circ \mathcal{N}_{\text{sat}}(u_c(k-q_1)) \\ \vdots \\ \mathcal{N} \circ \mathcal{N}_b \circ \mathcal{N}_s \circ \mathcal{N}_r \circ \mathcal{N}_{\text{sat}}(u_c(k-q_{l_{\tilde{U}}})) \end{bmatrix} \in \mathbb{R}^{l_{\tilde{U}}},$$

where for $i = 1, \ldots, l_{\tilde{U}}$, $k_1 \le q_i \le k_s + \ell$, and $\tilde{\mathcal{H}} \in \mathbb{R}^{s \times l_{\tilde{U}}}$ is constructed according to the structure of $\tilde{U}(k-1)$.

Next, for $j = 1, \ldots, s$, we define the *retrospective performance:*

$$\hat{z}_j(k-k_j) \triangleq \mathcal{S}_j(k-k_j) + \mathcal{H}_j \hat{U}_j(k-k_j-1), \quad (13)$$

where the past controls $U_j(k-k_j-1)$ in Equation (10) are replaced by the retrospective controls $\hat{U}_j(k-k_j-1)$. In analogy with Equation (11), the *extended retrospective performance* for Equation (13) is defined as

$$\hat{Z}(k) \triangleq \begin{bmatrix} \hat{z}_1(k-k_1) \\ \vdots \\ \hat{z}_s(k-k_s) \end{bmatrix} \in \mathbb{R}^s$$

and thus is given by

$$\hat{Z}(k) = \tilde{\mathcal{S}}(k) + \tilde{\mathcal{H}}\hat{\tilde{U}}(k-1), \quad (14)$$

where the components of $\hat{\tilde{U}}(k-1) \in \mathbb{R}^{l_{\tilde{U}}}$ are the components of $\hat{U}_1(k-k_1-1), \ldots, \hat{U}_s(k-k_s-1)$ ordered in the same way as the components of $\tilde{U}(k-1)$. Subtracting Equation (12) from Equation (14) yields

$$\hat{Z}(k) = Z(k) - \tilde{\mathcal{H}}\tilde{U}(k-1) + \tilde{\mathcal{H}}\hat{\tilde{U}}(k-1). \quad (15)$$

Finally, we define the *retrospective cost function:*

$$J(\hat{\tilde{U}}(k-1), k) \triangleq \hat{Z}^T(k) R(k) \hat{Z}(k), \quad (16)$$

where $R(k) \in \mathbb{R}^{s \times s}$ is a positive-definite performance weighting. The goal is to determine retrospectively optimised controls $\hat{\tilde{U}}(k-1)$ that would have provided better performance than the controls $U(k)$ that were applied to the system. The retrospectively optimised control values $\hat{\tilde{U}}(k-1)$ are subsequently used to update the controller.

Next, to ensure that Equation (16) has a global minimiser, we consider the regularised cost:

$$\bar{J}(\hat{\tilde{U}}(k-1), k) \triangleq \hat{Z}^T(k) R(k) \hat{Z}(k) + \eta(k) \hat{\tilde{U}}^T(k-1) \hat{\tilde{U}}(k-1), \quad (17)$$

where $\eta(k) \ge 0$. Substituting Equation (15) into Equation (17) yields

$$\bar{J}(\hat{\tilde{U}}(k-1), k) = \hat{\tilde{U}}(k-1)^T \mathcal{A}(k) \hat{\tilde{U}}(k-1) + \mathcal{B}(k) \hat{\tilde{U}}(k-1) + \mathcal{C}(k),$$

where

$$\mathcal{A}(k) \triangleq \tilde{\mathcal{H}}^T R(k) \tilde{\mathcal{H}} + \eta(k) I_{l_{\tilde{U}}},$$

$$\mathcal{B}(k) \triangleq 2\tilde{\mathcal{H}}^T R(k)[Z(k) - \tilde{\mathcal{H}}\tilde{U}(k-1)],$$

$$\mathcal{C}(k) \triangleq Z^T(k) R(k) Z(k) - 2Z^T(k) R(k) \tilde{\mathcal{H}} \tilde{U}(k-1) + \tilde{U}^T(k-1) \tilde{\mathcal{H}}^T R(k) \tilde{\mathcal{H}} \tilde{U}(k-1).$$

If either $\tilde{\mathcal{H}}$ has full column rank or $\eta(k) > 0$, then $\mathcal{A}(k)$ is positive definite. In this case, $\bar{J}(\hat{\tilde{U}}(k-1), k)$ has the unique global minimiser:

$$\hat{\tilde{U}}(k-1) = -\frac{1}{2} \mathcal{A}^{-1}(k) \mathcal{B}(k). \quad (18)$$

Next, let d be a positive integer such that $\hat{\tilde{U}}(k-1)$ contains $\hat{u}(k-d)$, and define the cumulative cost function:

$$J_R(\theta, k) \triangleq \sum_{i=d+1}^{k} \lambda^{k-i} \| \theta(k) \phi(i-d-1) - \hat{u}(i-d) \|^2 + \lambda^k (\theta(k) - \theta_0) P_0^{-1} (\theta(k) - \theta_0)^T, \quad (19)$$

where $\|\cdot\|$ is the Euclidean norm and $\lambda \in (0, 1]$ is the forgetting factor. Minimising Equation (19) yields

$$\theta(k) = \theta(k-1) + \beta(k)[\phi^T(k-d) P(k-1) \cdot \phi(k-d-1) + \lambda]^{-1} P(k-1) \phi(k-d-1) \cdot [\theta(k-1)\phi(k-d-1) - \hat{u}(k-d)],$$

where $\beta(k)$ is either 0 or 1. The error covariance is updated by

$$P(k) = \beta(k)\lambda^{-1} P(k-1) + [1 - \beta(k)] P(k-1) - \beta(k)\lambda^{-1} P(k-1) \phi(k-d-1) \cdot [\phi^T(k-d-1) P(k-1) \phi(k-d) + \lambda]^{-1} \cdot \phi^T(k-d-1) P(k-1).$$

We initialise the error covariance matrix as $P(0) = \alpha I_{2n_c}$, where $\alpha > 0$. Note that when $\beta(k) = 0$, $\theta(k) = \theta(k-1)$, and $P(k) = P(k-1)$. Therefore, setting $\beta(k) = 0$ switches off the controller adaptation, and thus freezes the control gains. When $\beta(k) = 1$, the controller is allowed to adapt. The parameter $\beta(k)$ is used only for numerical examples to illustrate the effect of adaptation.

4. Auxiliary nonlinearities

In this section, we construct the auxiliary nonlinearities $\mathcal{N}_{\rm sat}, \mathcal{N}_b, \mathcal{N}_s$, and $\mathcal{N}_r$ in Figure 2 along with the required model information. $\mathcal{N}_{\rm sat}$ modifies u_c to obtain the regressor input $u_{\rm sat}$, while $\mathcal{N}_b$, $\mathcal{N}_s$, and $\mathcal{N}_r$ modify $u_{\rm sat}$ to produce the Hammerstein plant input u. The auxiliary nonlinearities $\mathcal{N}_b$, $\mathcal{N}_s$, and $\mathcal{N}_r$ are chosen such that the composite input nonlinearity $\mathcal{N} \circ \mathcal{N}_r \circ \mathcal{N}_s \circ \mathcal{N}_b$ is globally non-decreasing. To avoid unnecessary complications, we assume that $\mathcal{N} \circ \mathcal{N}_r \circ \mathcal{N}_s \circ \mathcal{N}_b$ is redefined at points of discontinuity to render it piecewise right continuous.

For the Hammerstein command-following problem, we assume that G is uncertain except for an estimate of a single non-zero Markov parameter. The input nonlinearity $\mathcal{N}$ is also uncertain, as described below.

4.1 Auxiliary saturation nonlinearity $\mathcal{N}_{\rm sat}$

The auxiliary saturation nonlinearity $\mathcal{N}_{\rm sat}$ is defined to be the saturation function $\mathrm{sat}_{p,q}$ given by

$$\mathcal{N}_{\rm sat}(u_{\rm c}) = \mathrm{sat}_{p,q}(u_{\rm c}) = \begin{cases} p, & \text{if} \quad u_{\rm c} < p \\ u_{\rm c}, & \text{if} \quad p \le u_{\rm c} \le q \\ q, & \text{if} \quad u_{\rm c} > q, \end{cases} \tag{20}$$

where the real numbers p and q are the lower and upper saturation levels, respectively. For minimum-phase plants, the auxiliary nonlinearity $\mathcal{N}_{\rm sat}$ is not needed, and thus, in this case, the saturation levels p and q are chosen to be large negative and positive numbers, respectively. For NMP plants, the saturation levels are used to tune the transient behaviour. In addition, the saturation levels are chosen to provide a sufficiently large range of the control input to follow the command r. These values depend on the range of the input nonlinearity $\mathcal{N}$ as well as the gain of the linear system G at frequencies in the spectra of r and w.

4.2 Auxiliary reflection nonlinearity $\mathcal{N}_r$

If the input nonlinearity $\mathcal{N}$ is not monotonic, then the auxiliary reflection nonlinearity $\mathcal{N}_r$ is used to create a composite nonlinearity $\mathcal{N} \circ \mathcal{N}_r$ that is piecewise non-decreasing. To construct $\mathcal{N}_r$, we assume that the intervals of monotonicity of the input nonlinearity $\mathcal{N}$ are known, as described below.

In Sections 4.3 and 4.4, we restrict $\mathcal{N}_s$ and $\mathcal{N}_b$ so that $\mathcal{N}_s : [p, q] \to [p, q]$ and $\mathcal{N}_b : [p, q] \to [p, q]$. With this construction, we need to consider only $u_s \in [p, q]$. Therefore, let $I_1, I_2, \ldots$ be the smallest number of intervals of monotonicity of $\mathcal{N}$ that are a partition of the interval $[p, q]$. If $\mathcal{N}$ is non-decreasing on I_j, then $\mathcal{N}_r(u_s) \triangleq u_s$ for all $u_s \in I_i$. Alternatively, if $\mathcal{N}$ is non-increasing on $I_i = [p_i, q_i)$, then $\mathcal{N}_r(u_s) \triangleq p_i + q_i - u_s \in I_i$ for all $u_s \in I_i$. Finally, if $\mathcal{N}$ is constant on I_i, then either choice can be used. Thus, $\mathcal{N}_r$ is a piecewise-linear function that reflects $\mathcal{N}$ about $u_s = \frac{p_i+q_i}{2}$ within each interval of monotonicity so that $\mathcal{N} \circ \mathcal{N}_r$ is non-decreasing on I_i, and thus $\mathcal{N} \circ \mathcal{N}_r$ is piecewise non-decreasing on I. Let $\mathcal{R}_I(f)$ denote the range of the function f with arguments in I.

Proposition 4.1: *Assume that $\mathcal{N}_r$ is constructed by the above rule. Then, the following statements hold:*

(*i*) $\mathcal{N} \circ \mathcal{N}_r$ *is piecewise non-decreasing on* $[p, q]$;
(*ii*) $\mathcal{R}_I(\mathcal{N} \circ \mathcal{N}_r) = \mathcal{R}_I(\mathcal{N})$.

Proof: Let $I_i = (p_i, q_i)$. We first assume that $\mathcal{N}$ is non-decreasing on I_i. Since $\mathcal{N}_r(u_s) = u_s$ for all $u_s \in I_i$, it follows that $\mathcal{N} \circ \mathcal{N}_r(u_s) = \mathcal{N}(u_s)$ for all $u_s \in I_i$. Hence $\mathcal{N} \circ \mathcal{N}_r$ is non-decreasing on I_i and thus piecewise non-decreasing.

Alternatively, assume that $\mathcal{N}$ is non-increasing on I_i. Let $u_{s,1}, u_{s,2} \in I_i$, where $u_{s,1} \le u_{s,2}$. Then, $u_2 \triangleq p_i + q_i - u_{s,2} \le u_1 \triangleq p_i + q_i - u_{s,1}$. Therefore, since $\mathcal{N}$ is non-increasing on I_i, it follows that $\mathcal{N}(\mathcal{N}_r(u_{s,1})) = \mathcal{N}(u_1) \le \mathcal{N}(u_2) = \mathcal{N}(\mathcal{N}_r(u_{s,2}))$. Thus, $\mathcal{N} \circ \mathcal{N}_r$ is non-decreasing on I_i.

To prove (*ii*), assume that $\mathcal{N}$ is non-decreasing on I_i. Since $\mathcal{N}_r(u_s) = u_s$ for all $u_s \in I_i$, it follows that $\mathcal{N}_r(I_i) = I_i$, that is, $\mathcal{N}_r : I_i \to I_i$ is onto. Alternatively, assume that $\mathcal{N}$ is non-increasing on I_i so that $\mathcal{N}_r(u_s) = p_i + q_i - u_s$. Note that $\mathcal{N}_r(p_i) = q_i$, $\mathcal{N}_r(q_i) = p_i$, and $\mathcal{N}_r$ is continuous and decreasing on I_i. Therefore, $\mathcal{N}_r(I_i) = I_i$, and thus $\mathcal{N}_r : I_i \to I_i$ is onto. Hence, $\mathcal{R}_I(\mathcal{N} \circ \mathcal{N}_r) = \mathcal{R}_I(\mathcal{N})$. □

Example 4.2: Consider the non-increasing input nonlinearity $\mathcal{N}(u) = -\mathrm{sat}_{-1,1}(u - 5)$ shown in Figure 3(a). Let $\mathcal{N}_r(u_s) = -u_s + 10$ for all $u_s \in [3, 7]$ according to Proposition 4.1. Figure 3(c) shows that the composite nonlinearity $\mathcal{N} \circ \mathcal{N}_r$ is non-decreasing on $I \triangleq [3, 7]$. Note that $\mathcal{R}_I(\mathcal{N} \circ \mathcal{N}_r) = \mathcal{R}_I(\mathcal{N}) = [-1, 1]$.

Example 4.3: Consider the non-monotonic input nonlinearity $\mathcal{N}(u) = |u - 5|$ shown in Figure 4(a). Let $\mathcal{N}_r(u_s) = -u_s + 6$ for all $u_s \in [1, 5)$ and $\mathcal{N}_r(u_s) = u_s$, otherwise according to Proposition 4.1. Figure 4(c) shows that the composite nonlinearity $\mathcal{N} \circ \mathcal{N}_r$ is piecewise non-decreasing but not globally non-decreasing on $I \triangleq [1, 9]$, and that $\mathcal{R}_I(\mathcal{N} \circ \mathcal{N}_r) = \mathcal{R}_I(\mathcal{N}) = [0, 4]$.

Example 4.4: Consider the non-monotonic input nonlinearity,

$$\mathcal{N}(u) = \begin{cases} -\frac{1}{2}u, & \text{if } u \le 0 \\ u - 1, & \text{if } u > 0 \end{cases} \tag{21}$$

shown in Figure 5(a). Let $\mathcal{N}_r(u_s) = -u_s - 2$ for all $u_s \in [-2, 0)$ and $\mathcal{N}_r(u_s) = u_s$, otherwise according to

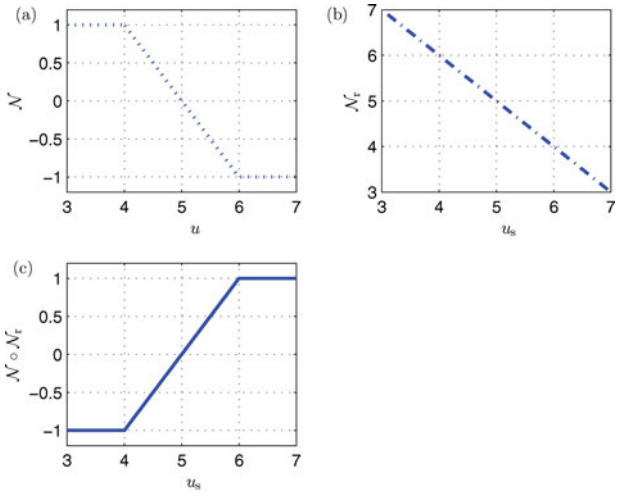

Figure 3. Example 4.2. (a) Input nonlinearity $\mathcal{N}(u) = -\text{sat}_{-1,1}(u-5)$. (b) Auxiliary reflection nonlinearity $\mathcal{N}_r(u_s) = -u_s + 10$ for $u_s \in [3, 7]$. (c) Composite nonlinearity $\mathcal{N} \circ \mathcal{N}_r$. Note that $\mathcal{N} \circ \mathcal{N}_r$ is non-decreasing on $I \triangleq [3, 7]$ and $\mathcal{R}_I(\mathcal{N} \circ \mathcal{N}_r) = \mathcal{R}_I(\mathcal{N}) = [-1, 1]$.

Proposition 4.1. Figure 5(c) shows that the composite nonlinearity $\mathcal{N} \circ \mathcal{N}_r$ is piecewise non-decreasing but not globally non-decreasing on $I \triangleq [-2, 1]$, and that $\mathcal{R}_I(\mathcal{N} \circ \mathcal{N}_r) = \mathcal{R}_I(\mathcal{N}) = [-1, 1]$.

4.3 *Auxiliary sorting nonlinearity $\mathcal{N}_s$*

As illustrated by Examples 4.3 and 4.4, $\mathcal{N} \circ \mathcal{N}_r$ is piecewise non-decreasing, but not globally non-decreasing. To construct a composite input nonlinearity that is globally

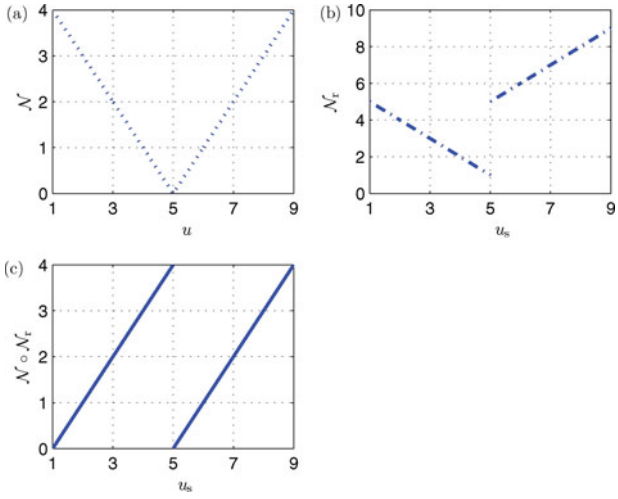

Figure 4. Example 4.3 (a) Non-monotonic input nonlinearity $\mathcal{N}(u) = -|u-5|$. (b) Auxiliary reflection nonlinearity $\mathcal{N}_r(u_s) = -u_s + 6$ for $u_s \in [1, 5)$, and $\mathcal{N}_r(u_s) = u_s$ otherwise. (c) Composite nonlinearity $\mathcal{N} \circ \mathcal{N}_r$. Note that $\mathcal{N} \circ \mathcal{N}_r$ is piecewise non-decreasing but not globally non-decreasing on $I \triangleq [1, 9]$, and that $\mathcal{R}_I(\mathcal{N} \circ \mathcal{N}_r) = \mathcal{R}_I(\mathcal{N}) = [0, 4]$.

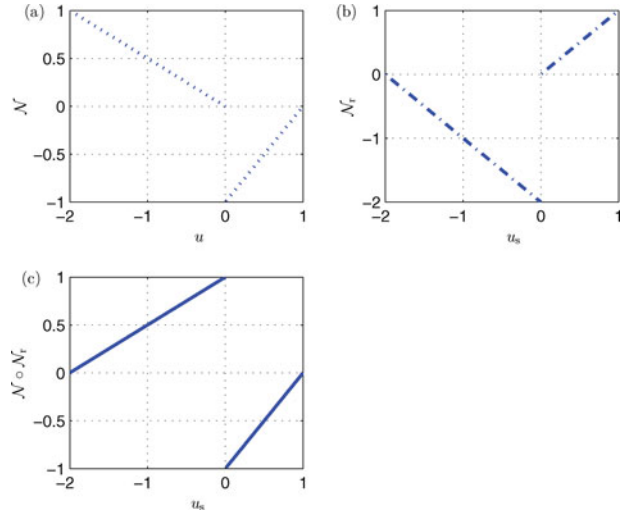

Figure 5. Example 4.4 (a) Non-monotonic input nonlinearity (21). (b) Auxiliary reflection nonlinearity $\mathcal{N}_r(u_s) = -u_s - 2$ for $u_s \in [-2, 0)$ and $\mathcal{N}_r(u_s) = u_s$ otherwise. (c) Composite nonlinearity $\mathcal{N} \circ \mathcal{N}_r$. Note that $\mathcal{N} \circ \mathcal{N}_r$ is piecewise non-decreasing but not globally non-decreasing on $I \triangleq [-2, 0]$, and that $\mathcal{R}_I(\mathcal{N} \circ \mathcal{N}_r) = \mathcal{R}_I(\mathcal{N}) = [-1, 1]$.

non-decreasing, we introduce the auxiliary sorting nonlinearity $\mathcal{N}_s$ and auxiliary blocking nonlinearity $\mathcal{N}_b$. The auxiliary sorting nonlinearity $\mathcal{N}_s$ sorts portions of the piecewise non-decreasing nonlinearity $\mathcal{N} \circ \mathcal{N}_r$ to create a composite nonlinearity $\mathcal{N} \circ \mathcal{N}_r \circ \mathcal{N}_s$, so that the composite nonlinearity $\mathcal{N} \circ \mathcal{N}_r \circ \mathcal{N}_s \circ \mathcal{N}_b$ is globally non-decreasing. $\mathcal{N}_b$ is discussed in Section 4.4. To construct $\mathcal{N}_s$, we assume that the range of $\mathcal{N} \circ \mathcal{N}_r$ within each interval of monotonicity is known. No further modelling information about $\mathcal{N}$ is needed.

Let $\mathcal{N}_s$ be the piecewise right-continuous affine function defined as follows. Let $I_1 = [p_1, q_1)$, $I_2 = [p_2, q_2)$, ... be the smallest number of intervals of monotonicity of $\mathcal{N}$ that are a partition of the interval $[p, q]$. If $\mathcal{R}_{I_i}(\mathcal{N} \circ \mathcal{N}_r) \subset \mathcal{R}_{I_j}(\mathcal{N} \circ \mathcal{N}_r)$ for all $i \neq j$ or $(\mathcal{N} \circ \mathcal{N}_r)(q_i) \leq (\mathcal{N} \circ \mathcal{N}_r)(q_j)$, where $q_i < q_j$, then $\mathcal{N}_s(u_b) \triangleq u_b$ for all $u_b \in I_i \cup I_j = [p_i, q_i) \cup [p_j, q_j)$, and thus $\mathcal{N}_s$ is not needed. Alternatively, if $\mathcal{R}_{I_i}(\mathcal{N} \circ \mathcal{N}_r) \nsubseteq \mathcal{R}_{I_j}(\mathcal{N} \circ \mathcal{N}_r)$ for all $i \neq j$ and $(\mathcal{N} \circ \mathcal{N}_r)(q_i) > (\mathcal{N} \circ \mathcal{N}_r)(q_j)$, where $q_i < q_j$, then $\mathcal{N}_s(u_b) \triangleq \frac{1}{q_i - p_i}[(q_j - p_j)u_b + p_j q_i - p_i q_j] \in I_j$ for all $u_b \in I_i$ and $\mathcal{N}_s(u_b) \triangleq \frac{1}{q_j - p_j}[(q_i - p_i)u_b + p_i q_j - p_j q_i] \in I_i$ for all $u_b \in I_j$.

Proposition 4.5: *Assume that $\mathcal{N}_s$ is constructed by the above rule. Then, the following statements hold:*

(*i*) $\mathcal{N} \circ \mathcal{N}_r \circ \mathcal{N}_s$ *is piecewise non-decreasing on* $[p, q]$;
(*ii*) $\mathcal{R}_I(\mathcal{N} \circ \mathcal{N}_r \circ \mathcal{N}_s) = \mathcal{R}_I(\mathcal{N})$.

Proof: Let $I_i = (p_i, q_i)$ and $I_j = (p_j, q_j)$. We first assume that $\mathcal{R}_{I_i}(\mathcal{N} \circ \mathcal{N}_r) \subset \mathcal{R}_{I_j}(\mathcal{N} \circ \mathcal{N}_r)$ for all $i \neq j$ or $\mathcal{N} \circ \mathcal{N}_r(q_i) \leq \mathcal{N} \circ \mathcal{N}_r(q_j)$, where $q_i < q_j$. Since $\mathcal{N}_s(u_b) = u_b$ for all $u_b \in$

$I_i \cup I_j$, it follows from Proposition 4.1 (i) that $\mathcal{N} \circ \mathcal{N}_r \circ \mathcal{N}_s$ is piecewise non-decreasing on $[p, q]$.

Alternatively, assume that $\mathcal{R}_{I_i}(\mathcal{N} \circ \mathcal{N}_r) \not\subseteq \mathcal{R}_{I_j}(\mathcal{N} \circ \mathcal{N}_r)$ for all $i \neq j$ and $(\mathcal{N} \circ \mathcal{N}_r)(q_i) > (\mathcal{N} \circ \mathcal{N}_r)(q_j)$, where $q_i < q_j$. It follows from $\mathcal{N}_s(u_b) \triangleq \frac{1}{q_i - p_i}[(q_j - p_j)u_b + p_j q_i - p_i q_j] \in I_j$ for all $u_b \in I_i$ and $\mathcal{N}_s(u_b) \triangleq \frac{1}{q_j - p_j}[(q_i - p_i)u_b + p_i q_j - p_j q_i] \in I_i$ for all $u_b \in I_j$ that $\mathcal{N}_s : I_i \to I_j$ and $\mathcal{N}_s : I_j \to I_i$. Next, let $u_{b,1}, u_{b,2} \in I_i$, where $u_{b,1} \leq u_{b,2}$. Then,

$$u_{s,1} \triangleq \frac{1}{q_i - p_i}[(q_j - p_j)u_{b,1} + p_j q_i - p_i q_j] \in I_j \leq u_{s,2} \triangleq \frac{1}{q_i - p_i}[(q_j - p_j)u_{b,2} + p_j q_i - p_i q_j] \in I_j.$$

Therefore, since $\mathcal{N} \circ \mathcal{N}_r$ is non-decreasing on I_j, it follows that $(\mathcal{N} \circ \mathcal{N}_r \circ \mathcal{N}_s)(u_{b,1}) = (\mathcal{N} \circ \mathcal{N}_r)(u_{s,1}) \leq (\mathcal{N} \circ \mathcal{N}_r)(u_{s,2}) = (\mathcal{N} \circ \mathcal{N}_r \circ \mathcal{N}_s)(u_{b,2})$. Thus, $\mathcal{N} \circ \mathcal{N}_r \circ \mathcal{N}_s$ is non-decreasing on I_i. Similarly, the same argument shows that $\mathcal{N} \circ \mathcal{N}_r \circ \mathcal{N}_s$ is non-decreasing on I_j.

To prove (ii), assume that $\mathcal{R}_{I_i}(\mathcal{N} \circ \mathcal{N}_r) \subset \mathcal{R}_{I_j}(\mathcal{N} \circ \mathcal{N}_r)$ for all $i \neq j$ or $(\mathcal{N} \circ \mathcal{N}_r)(q_i) \leq (\mathcal{N} \circ \mathcal{N}_r)(q_j)$, where $q_i < q_j$. Since $\mathcal{N}_s(u_b) = u_b$ for all $u_b \in I_i \cup I_j$, it follows that $\mathcal{N}_s : I_i \to I_i$ is onto. Alternatively, assume that $\mathcal{R}_{I_i}(\mathcal{N} \circ \mathcal{N}_r) \not\subseteq \mathcal{R}_{I_j}(\mathcal{N} \circ \mathcal{N}_r)$ for all $i \neq j$ and $\mathcal{N} \circ \mathcal{N}_r(q_i) > \mathcal{N} \circ \mathcal{N}_r(q_j)$, where $q_i < q_j$. It follows from $\mathcal{N}_s(u_b) \triangleq \frac{1}{q_i - p_i}[(q_j - p_j)u_b + p_j q_i - p_i q_j] \in I_j$ for all $u_b \in I_i$ and $\mathcal{N}_s(u_b) \triangleq \frac{1}{q_j - p_j}[(q_i - p_i)u_b + p_i q_j - p_j q_i] \in I_i$ for all $u_b \in I_j$ that $\mathcal{N}_s : I_i \to I_j$ and $\mathcal{N}_s : I_j \to I_i$. Therefore, $\mathcal{N}_s : I_i \to I_j$ and $\mathcal{N}_s : I_j \to I_i$. Hence, $\mathcal{R}_I(\mathcal{N} \circ \mathcal{N}_r \circ \mathcal{N}_s) = \mathcal{R}_I(\mathcal{N} \circ \mathcal{N}_r) = \mathcal{R}_I(\mathcal{N})$. □

Example 4.6: Consider the case where $\mathcal{R}_{[-2,0]}(\mathcal{N} \circ \mathcal{N}_r) \cap \mathcal{R}_{[0,1]}(\mathcal{N} \circ \mathcal{N}_r) = \varnothing$ as shown in Figure 6(a). We assume that values of $(\mathcal{N} \circ \mathcal{N}_r)(0)$ and $(\mathcal{N} \circ \mathcal{N}_r)(1)$ are known. In particular, $(\mathcal{N} \circ \mathcal{N}_r)(0) = 1 > (\mathcal{N} \circ \mathcal{N}_r)(1) = 0$. We thus choose $\mathcal{N}_s(u_b) = 0.5u_b + 1$ for $u_b \in [-2, 0)$ and $\mathcal{N}_s(u_b) = 2u_b - 2$ for $u_b \in [0, 1]$ as shown in Figure 6(b). Note that $\mathcal{N} \circ \mathcal{N}_r$ is piecewise non-decreasing on $[-2, 1]$. Figure 6(c) shows that the composite nonlinearity $\mathcal{N} \circ \mathcal{N}_r \circ \mathcal{N}_s$ is piecewise non-decreasing on $[-2, 1]$.

Example 4.7: Consider the case where range of $\mathcal{N} \circ \mathcal{N}_r$ on subintervals of its domain has partially overlapping intervals as shown in Figure 7(a), where neither $\mathcal{R}_{[-5,0]}(\mathcal{N} \circ \mathcal{N}_r)$ nor $\mathcal{R}_{[0,5]}(\mathcal{N} \circ \mathcal{N}_r)$ is contained in the other set. We assume that values of $(\mathcal{N} \circ \mathcal{N}_r)(0)$ and $(\mathcal{N} \circ \mathcal{N}_r)(5)$ are known. In particular, $(\mathcal{N} \circ \mathcal{N}_r)(0) = 4 > (\mathcal{N} \circ \mathcal{N}_r)(5) = 1$, we thus choose $\mathcal{N}_s(u_b) = u_b + 5$ for $u_b \in [-5, 0)$ and $\mathcal{N}_s(u_b) = u_b - 5$ for $u_b \in [0, 5]$ as shown in Figure 7(b). Note that $\mathcal{N} \circ \mathcal{N}_r \circ \mathcal{N}_s$ is piecewise non-decreasing on $[-5, 5]$, and Figure 7(c) shows that the composite nonlinearity $\mathcal{N} \circ \mathcal{N}_r \circ \mathcal{N}_s$ is piecewise non-decreasing on $[-5, 5]$.

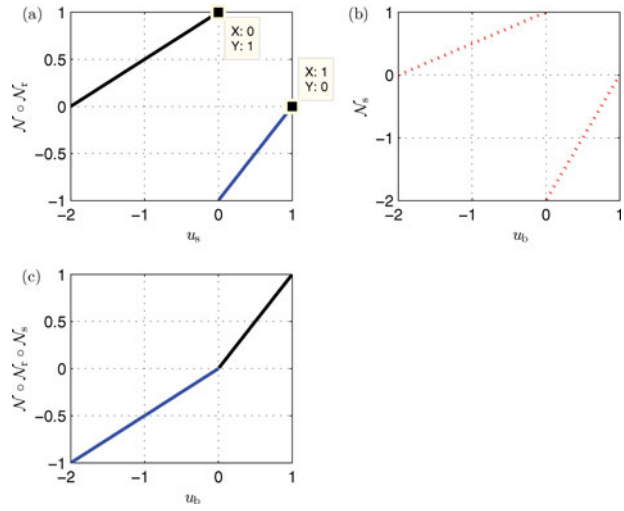

Figure 6. Example 4.6. In this example, $\mathcal{R}_{[-2,0]}(\mathcal{N} \circ \mathcal{N}_r) \cap \mathcal{R}_{[0,1]}(\mathcal{N} \circ \mathcal{N}_r) = \varnothing$. (a) Non-decreasing composite nonlinearity $\mathcal{N} \circ \mathcal{N}_r$. Note that $(\mathcal{N} \circ \mathcal{N}_r)(0) = 1 > (\mathcal{N} \circ \mathcal{N}_r)(1) = 0$. (b) Auxiliary sorting nonlinearity $\mathcal{N}_s(u_b) = 0.5u_b + 1$ for $u_b \in [-2, 0)$ and $\mathcal{N}_s(u_b) = 2u_b - 2$ for $u_b \in [0, 1]$. (c) The composite nonlinearity $\mathcal{N} \circ \mathcal{N}_r \circ \mathcal{N}_s$.

Example 4.8: Consider the case where $\mathcal{R}_{[-5,0]}(\mathcal{N} \circ \mathcal{N}_r) \subset \mathcal{R}_{[0,5]}(\mathcal{N} \circ \mathcal{N}_r)$ as shown in Figure 8(a), and thus $\mathcal{N}_s$ is not needed. We choose $\mathcal{N}_s(u_b) = u_b$, and Figure 8(b) shows that $\mathcal{N} \circ \mathcal{N}_r \circ \mathcal{N}_s$ is piecewise non-decreasing on $[-5, 5]$.

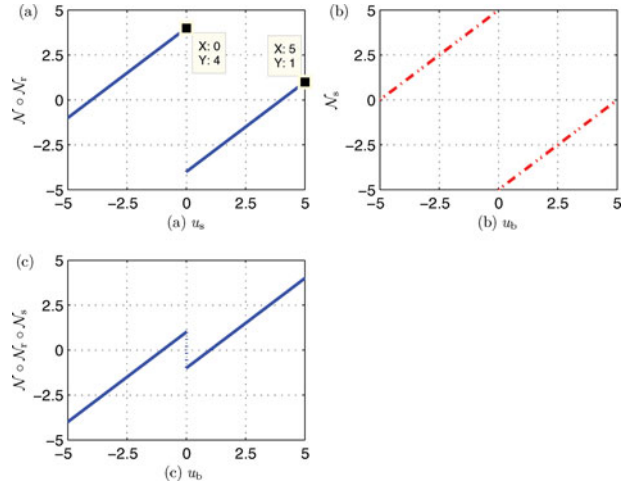

Figure 7. Example 4.7. In this example, range of $\mathcal{N} \circ \mathcal{N}_r$ on subintervals of its domain has partially overlapping intervals, where neither $\mathcal{R}_{[-5,0]}(\mathcal{N} \circ \mathcal{N}_r)$ nor $\mathcal{R}_{[0,5]}(\mathcal{N} \circ \mathcal{N}_r)$ is contained in the other set. Note that $(\mathcal{N} \circ \mathcal{N}_r)(0) = 4 > (\mathcal{N} \circ \mathcal{N}_r)(5) = 1$. (a) Piecewise non-decreasing composite nonlinearity $\mathcal{N} \circ \mathcal{N}_r$ with partially overlapping intervals. (b) Auxiliary sorting nonlinearity $\mathcal{N}_s(u_b) = u_b + 5$ for $u_b \in [-5, 0)$ and $\mathcal{N}_s(u_b) = u_b - 5$ for $u_b \in [0, 5]$. (c) The composite nonlinearity $\mathcal{N} \circ \mathcal{N}_r \circ \mathcal{N}_s$ is piecewise non-decreasing on $[-5, 5]$.

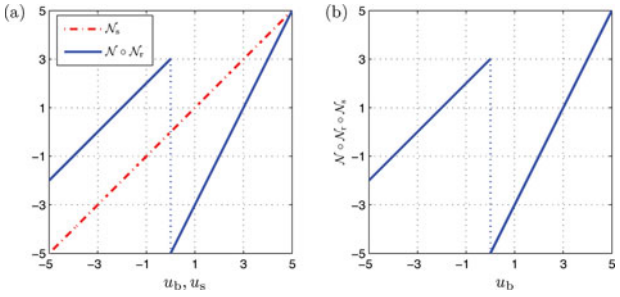

Figure 8. Example 4.8. In this example, $\mathcal{R}_{[-5,0]}(\mathcal{N} \circ \mathcal{N}_r) \subset \mathcal{R}_{[0,5]}(\mathcal{N} \circ \mathcal{N}_r)$. In this case, $\mathcal{N}_s$ is not needed. (a) Piecewise non-decreasing composite nonlinearity $\mathcal{N} \circ \mathcal{N}_r$, where $\mathcal{R}_{[-5,0]}(\mathcal{N} \circ \mathcal{N}_r) \subset \mathcal{R}_{[0,5]}(\mathcal{N} \circ \mathcal{N}_r)$ and the auxiliary sorting nonlinearity $\mathcal{N}_s(u_b) = u_b$ for $u_b \in [-5, 5]$. (b) The composite nonlinearity $\mathcal{N} \circ \mathcal{N}_r \circ \mathcal{N}_s$ is piecewise non-decreasing on $[-5, 5]$.

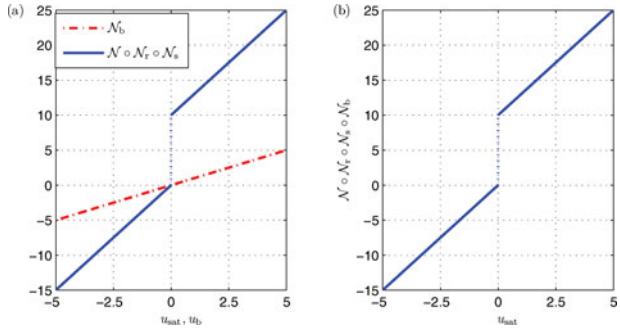

Figure 9. Example 4.9. In this example, $\mathcal{R}_{[-5,0]}(\mathcal{N} \circ \mathcal{N}_r \circ \mathcal{N}_s) \cap \mathcal{R}_{[0,5]}(\mathcal{N} \circ \mathcal{N}_r \circ \mathcal{N}_s) = \varnothing$. (a) Non-decreasing composite nonlinearity $\mathcal{N} \circ \mathcal{N}_r \circ \mathcal{N}_s$ and auxiliary blocking nonlinearity $\mathcal{N}_b(u_{\rm sat}) = u_{\rm sat}$. (b) The composite nonlinearity $\mathcal{N} \circ \mathcal{N}_r \circ \mathcal{N}_s \circ \mathcal{N}_b$ is globally non-decreasing on $[-5, 5]$.

4.4 *Auxiliary blocking nonlinearity $\mathcal{N}_b$*

As shown in Proposition 4.5 and illustrated by Example 4.7, $\mathcal{N} \circ \mathcal{N}_r \circ \mathcal{N}_s$ is piecewise non-decreasing. To construct a composite input nonlinearity that is globally non-decreasing, we introduce the auxiliary blocking nonlinearity $\mathcal{N}_b$. To construct $\mathcal{N}_b$, we assume that the range of $\mathcal{N} \circ \mathcal{N}_r \circ \mathcal{N}_s$ within each interval of monotonicity is known. If, in addition, these ranges are partially overlapping, then selected intermediate values of $\mathcal{N} \circ \mathcal{N}_r \circ \mathcal{N}_s$ must be known. No further modelling information about $\mathcal{N}$ is needed.

Let $\mathcal{N}_b$ be the piecewise right-continuous affine function defined as follows. Let $I_1, I_2, \ldots$ be the smallest number of intervals of monotonicity of $\mathcal{N}$ that are also a partition of the interval $[p, q]$. If $\mathcal{R}_{I_i}(\mathcal{N} \circ \mathcal{N}_r \circ \mathcal{N}_s) \cap \mathcal{R}_{I_j}(\mathcal{N} \circ \mathcal{N}_r \circ \mathcal{N}_s) = \varnothing$ for all $i \neq j$, then we choose $\mathcal{N}_b(u_{\rm sat}) \stackrel{\triangle}{=} u_{\rm sat}$ for all $u_{\rm sat} \in I_j \cup I_j$. Alternatively, if $\mathcal{R}_{I_i}(\mathcal{N} \circ \mathcal{N}_r \circ \mathcal{N}_s) \cap \mathcal{R}_{I_j}(\mathcal{N} \circ \mathcal{N}_r \circ \mathcal{N}_s) \neq \varnothing$ and $\mathcal{R}_{I_i}(\mathcal{N} \circ \mathcal{N}_r \circ \mathcal{N}_s) \subsetneq \mathcal{R}_{I_j}(\mathcal{N} \circ \mathcal{N}_r \circ \mathcal{N}_s)$, we block the overlapping segments as shown by the following examples to illustrate three different cases where the subintervals have no overlapping intervals, partially overlapping intervals, and overlapping intervals.

Example 4.9: Consider the case where $\mathcal{R}_{[-5,0]}(\mathcal{N} \circ \mathcal{N}_r \circ \mathcal{N}_s) \cap \mathcal{R}_{[0,5]}(\mathcal{N} \circ \mathcal{N}_r \circ \mathcal{N}_s) = \varnothing$ as shown in Figure 9(a). In this case, $\mathcal{N}_b$ is not needed, we thus choose $\mathcal{N}_b(u_{\rm sat}) = u_{\rm sat}$. Note that $\mathcal{N} \circ \mathcal{N}_r \circ \mathcal{N}_s$ is piecewise non-decreasing on $[-5, 5]$. Figure 9(b) shows that the composite nonlinearity $\mathcal{N} \circ \mathcal{N}_r \circ \mathcal{N}_s \circ \mathcal{N}_b$ is globally non-decreasing on $[-5, 5]$.

Example 4.10: Consider the case where range of $\mathcal{N} \circ \mathcal{N}_r \circ \mathcal{N}_s$ on subintervals of its domain has partially overlapping intervals, where neither $\mathcal{R}_{[-5,0]}(\mathcal{N} \circ \mathcal{N}_r \circ \mathcal{N}_s)$ nor $\mathcal{R}_{[0,5]}(\mathcal{N} \circ \mathcal{N}_r \circ \mathcal{N}_s)$ is contained in the other set. In particular, as shown in Figure 10(a), $\mathcal{R}_{[-2,0]}(\mathcal{N} \circ \mathcal{N}_r \circ \mathcal{N}_s) = \mathcal{R}_{[0,2]}(\mathcal{N} \circ \mathcal{N}_r \circ \mathcal{N}_s)$. In this case, we assume that intermediate values of $\mathcal{N} \circ \mathcal{N}_r \circ \mathcal{N}_s$ are known. In particular, knowledge of $(\mathcal{N} \circ \mathcal{N}_r \circ \mathcal{N}_s)_{[-5,0]}(0) = 1$ is sufficient to construct $\mathcal{N}_b$. We choose $\mathcal{N}_b(u_{\rm sat}) = -2$ for $u_{\rm sat} \in [-2, 0)$ and $\mathcal{N}_b(u_{\rm sat}) = u_{\rm sat}$, otherwise. Note that $\mathcal{N} \circ \mathcal{N}_r \circ \mathcal{N}_s$ is piecewise non-decreasing on $[-5, 5]$, and Figure 10(b) shows that the composite nonlinearity $\mathcal{N} \circ \mathcal{N}_r \circ \mathcal{N}_s \circ \mathcal{N}_b$ is globally non-decreasing on $[-5, 5]$.

Example 4.11: Consider the case $\mathcal{R}_{[-5,0]}(\mathcal{N} \circ \mathcal{N}_r \circ \mathcal{N}_s) \subset \mathcal{R}_{[0,5]}(\mathcal{N} \circ \mathcal{N}_r \circ \mathcal{N}_s)$ as shown in Figure 11(a). In particular, $\mathcal{R}_{[-5,0]}(\mathcal{N} \circ \mathcal{N}_r \circ \mathcal{N}_s) = [-2, 3]$ and $\mathcal{R}_{[0,5]}(\mathcal{N} \circ \mathcal{N}_r \circ \mathcal{N}_s) = [-5, 5]$. We let $\mathcal{N}_b(u_{\rm sat}) = -5$ for all $u_{\rm sat} \in [-5, 0)$ and $\mathcal{N}_b(u_{\rm sat}) = u_{\rm sat}$ for all $u_{\rm sat} \in [0, 5]$. Note that $\mathcal{N} \circ \mathcal{N}_r \circ \mathcal{N}_s$ is piecewise non-decreasing on $[-5, 5]$ and Figure 11(b) shows that the composite nonlinearity $\mathcal{N} \circ \mathcal{N}_r \circ \mathcal{N}_s \circ \mathcal{N}_b$ is globally non-decreasing on $[-5, 5]$.

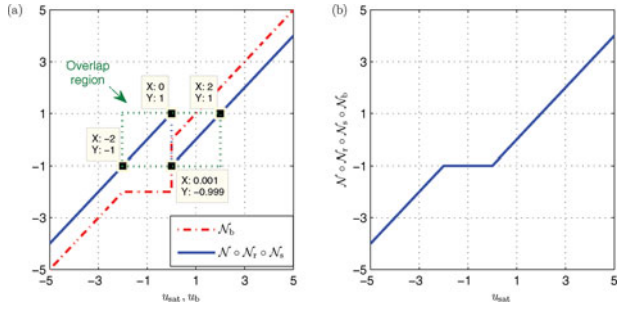

Figure 10. Example 4.10. In this example, range of $\mathcal{N} \circ \mathcal{N}_r \circ \mathcal{N}_s$ on subintervals of its domain has partially overlapping intervals, where neither $\mathcal{R}_{[-5,0]}(\mathcal{N} \circ \mathcal{N}_r \circ \mathcal{N}_s)$ nor $\mathcal{R}_{[0,5]}(\mathcal{N} \circ \mathcal{N}_r \circ \mathcal{N}_s)$ is contained in the other set. (a) Piecewise non-decreasing composite nonlinearity $\mathcal{N} \circ \mathcal{N}_r \circ \mathcal{N}_s$ with partially overlapping intervals, where $\mathcal{R}_{[-2,0]}(\mathcal{N} \circ \mathcal{N}_r \circ \mathcal{N}_s) = \mathcal{R}_{[0,2]}(\mathcal{N} \circ \mathcal{N}_r \circ \mathcal{N}_s)$ and the auxiliary blocking nonlinearity $\mathcal{N}_b(u_{\rm sat}) = u_{\rm sat}$. (b) The composite nonlinearity $\mathcal{N} \circ \mathcal{N}_r \circ \mathcal{N}_s \circ \mathcal{N}_b$ is globally non-decreasing on $[-5, 5]$.

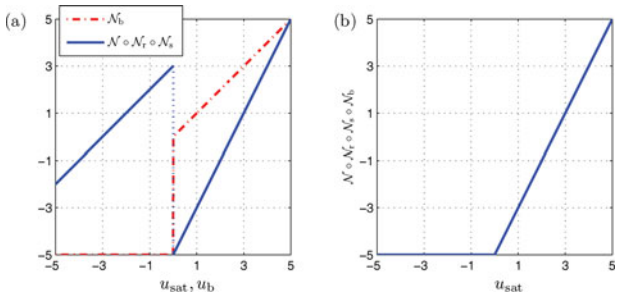

Figure 11. Example 4.11. In this example, $\mathcal{R}_{[-5,0]}(\mathcal{N}\circ\mathcal{N}_r\circ\mathcal{N}_s)\subset\mathcal{R}_{[0,5]}(\mathcal{N}\circ\mathcal{N}_r\circ\mathcal{N}_s)$. (a) Piecewise non-decreasing composite nonlinearity $\mathcal{N}\circ\mathcal{N}_r\circ\mathcal{N}_s$, where $\mathcal{R}_{[-5,0]}(\mathcal{N}\circ\mathcal{N}_r\circ\mathcal{N}_s)\subset\mathcal{R}_{[0,5]}(\mathcal{N}\circ\mathcal{N}_r\circ\mathcal{N}_s)$ and the auxiliary blocking nonlinearity $\mathcal{N}_b(u_{\text{sat}})=-5$ for $u_{\text{sat}}\in[-5,0)$ and $\mathcal{N}_b(u_{\text{sat}})=u_{\text{sat}}$ for $u_{\text{sat}}\in[0,5]$. (b) The composite nonlinearity $\mathcal{N}\circ\mathcal{N}_r\circ\mathcal{N}_s\circ\mathcal{N}_b$ is globally non-decreasing on $[-5,5]$.

Proposition 4.12: *Assume that $\mathcal{N}_b$ is constructed by the above rule. Then the following statements hold:*

(*i*) $\mathcal{N}\circ\mathcal{N}_r\circ\mathcal{N}_s\circ\mathcal{N}_b$ *is globally non-decreasing on* $I\stackrel{\triangle}{=}[p,q]$;
(*ii*) $\mathcal{R}_I(\mathcal{N}\circ\mathcal{N}_r\circ\mathcal{N}_s\circ\mathcal{N}_b)=\mathcal{R}_I(\mathcal{N})$.

Proof: First, consider the case $\mathcal{R}_{I_i}(\mathcal{N}\circ\mathcal{N}_r\circ\mathcal{N}_s)\cap\mathcal{R}_{I_j}(\mathcal{N}\circ\mathcal{N}_r\circ\mathcal{N}_s)=\varnothing$ for all $i\neq j$. It follows from (*i*) of Proposition 4.5 and $\mathcal{N}_b(u_{\text{sat}})=u_{\text{sat}}$ that $\mathcal{N}\circ\mathcal{N}_r\circ\mathcal{N}_s\circ\mathcal{N}_b$ is non-decreasing on I. Next, consider the case $\mathcal{R}_{I_i}(\mathcal{N}\circ\mathcal{N}_r\circ\mathcal{N}_s)\cap\mathcal{R}_{I_j}(\mathcal{N}\circ\mathcal{N}_r\circ\mathcal{N}_s)\neq\varnothing$, $(\mathcal{N}\circ\mathcal{N}_r\circ\mathcal{N}_s\circ\mathcal{N}_b)(u_{\text{sat}})$ is constant for all $u_{\text{sat}}\in\mathcal{R}_{I_i}(\mathcal{N}\circ\mathcal{N}_r\circ\mathcal{N}_s)\cap\mathcal{R}_{I_j}(\mathcal{N}\circ\mathcal{N}_r\circ\mathcal{N}_s)$. Therefore, $\mathcal{N}\circ\mathcal{N}_r\circ\mathcal{N}_s\circ\mathcal{N}_b$ is non-decreasing.

To prove (*ii*), let I_1, I_2, ... be the smallest number of intervals of monotonicity of $\mathcal{N}$ that are a partition of the interval $[p,q]$. Since $\mathcal{R}_I(\mathcal{N}\circ\mathcal{N}_r\circ\mathcal{N}_s)=\bigcup_{k=1}^{\infty}\mathcal{R}_{I_k}(\mathcal{N}\circ\mathcal{N}_r\circ\mathcal{N}_s)$. Note that $\mathcal{N}_b(u_{\text{sat}})=u_{\text{sat}}$ for all intervals I_i and I_j such that $\mathcal{R}_{I_i}(\mathcal{N}\circ\mathcal{N}_r\circ\mathcal{N}_s)\cap\mathcal{R}_{I_j}(\mathcal{N}\circ\mathcal{N}_r\circ\mathcal{N}_s)=\varnothing$. For the intervals where $\mathcal{R}_{I_i}(\mathcal{N}\circ\mathcal{N}_r\circ\mathcal{N}_s)\cap\mathcal{R}_{I_j}(\mathcal{N}\circ\mathcal{N}_r\circ\mathcal{N}_s)\neq\varnothing$. Let $\mathcal{N}_b(u_{\text{sat}})=\mu$, where $\mu\in\mathcal{R}_{I_i}(\mathcal{N}\circ\mathcal{N}_r\circ\mathcal{N}_s)\cap\mathcal{R}_{I_j}(\mathcal{N}\circ\mathcal{N}_r\circ\mathcal{N}_s)$. Therefore, $\mathcal{R}_I(\mathcal{N}\circ\mathcal{N}_r\circ\mathcal{N}_s\circ\mathcal{N}_b)=\mathcal{R}_I(\mathcal{N}\circ\mathcal{N}_r\circ\mathcal{N}_s)$. It thus follows from Proposition 4.5 that $\mathcal{R}_I(\mathcal{N}\circ\mathcal{N}_r\circ\mathcal{N}_s\circ\mathcal{N}_b)=\mathcal{R}_I(\mathcal{N}\circ\mathcal{N}_r\circ\mathcal{N}_s)=\mathcal{R}_I(\mathcal{N})$. □

4.5 *Examples illustrating the construction of $\mathcal{N}_b$, $\mathcal{N}_s$, and $\mathcal{N}_r$*

Example 4.13: Consider the non-monotonic input nonlinearity:

$$\mathcal{N}(u)=\begin{cases}10, & \text{if } u<2\\ -3u+4, & \text{if } -2\le u<2\\ u^2-6, & \text{if } u\ge 2,\end{cases}\tag{22}$$

which is shown in Figure 12(a). Let $\mathcal{N}_{\text{sat}}(u_c)=\text{sat}_{p,q}(u_c)$, where $p=-5$ and $q=5$. According to Propositions 4.1, 4.5, and 4.12, let

$$\mathcal{N}_r(u_s)=\begin{cases}-u_s, & \text{if } -2\le u_s<2\\ u_s, & \text{if } u_s\in[-5,-2)\cup(2,5),\end{cases}\tag{23}$$

$$\mathcal{N}_s(u_b)=u_b,\quad \text{if } u_b\in[-5,5],\tag{24}$$

and

$$\mathcal{N}_b(u_{\text{sat}})=\begin{cases}-2, & \text{if } -5\le u_{\text{sat}}<2\\ u_{\text{sat}}, & \text{if } 2\le u_{\text{sat}}\le 5.\end{cases}\tag{25}$$

Figure 12(b) shows the auxiliary nonlinearities $\mathcal{N}_b$, $\mathcal{N}_s$, and $\mathcal{N}_r$. Figure 12(c) and 12(d) show that the composite nonlinearity $\mathcal{N}\circ\mathcal{N}_r\circ\mathcal{N}_s$ is piecewise non-decreasing on $I\stackrel{\triangle}{=}[-5,5]$ and the composite nonlinearity $\mathcal{N}\circ\mathcal{N}_r\circ\mathcal{N}_s\circ\mathcal{N}_b$ is globally non-decreasing on I. Note that $\mathcal{R}_I(\mathcal{N}\circ\mathcal{N}_r\circ\mathcal{N}_s\circ\mathcal{N}_b)=\mathcal{R}_I(\mathcal{N})=[-2,19]$.

Example 4.14: Consider the non-monotonic input nonlinearity:

$$\mathcal{N}(u)=\begin{cases}-\text{sat}_{-0.5,0.5}u, & \text{if } u<2\\ 0.5u-2, & \text{if } 2\le u<4\\ 0, & \text{if } u\ge 4,\end{cases}\tag{26}$$

which is shown in Figure 13(a). Let $\mathcal{N}_{\text{sat}}(u_c)=\text{sat}_{p,q}(u_c)$, where $p=-2$ and $q=6$. According to Propositions 4.1, 4.5, and 4.12, let

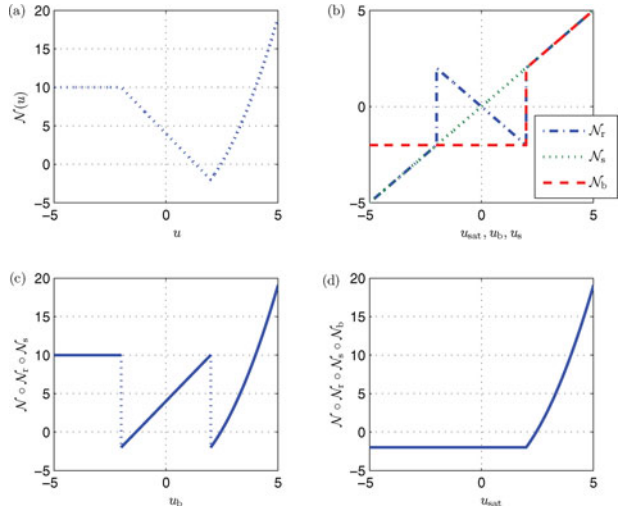

Figure 12. Example 4.13. (a) Input nonlinearity given by Equation (22). (b) The auxiliary reflection nonlinearity $\mathcal{N}_r$ given by Equation (23) for $u_s\in[-5,5]$, the auxiliary sorting nonlinearity $\mathcal{N}_s$ given by Equation (24) for $u_b\in[-5,5]$, and the auxiliary blocking nonlinearity $\mathcal{N}_b$ given by Equation (25) for $u_{\text{sat}}\in[-5,5]$. (c) Composite nonlinearity $\mathcal{N}\circ\mathcal{N}_r\circ\mathcal{N}_s$. Note that $\mathcal{N}\circ\mathcal{N}_r\circ\mathcal{N}_s$ is piecewise non-decreasing on $[-5,5]$. (d) Composite nonlinearity $\mathcal{N}\circ\mathcal{N}_r\circ\mathcal{N}_s\circ\mathcal{N}_b$. Note that $\mathcal{N}\circ\mathcal{N}_r\circ\mathcal{N}_s\circ\mathcal{N}_b$ is globally non-decreasing on $[-5,5]$ and $\mathcal{R}_{[-5,5]}(\mathcal{N}\circ\mathcal{N}_r\circ\mathcal{N}_s\circ\mathcal{N}_b)=\mathcal{R}_{[-5,5]}(\mathcal{N})=[-2,19]$.

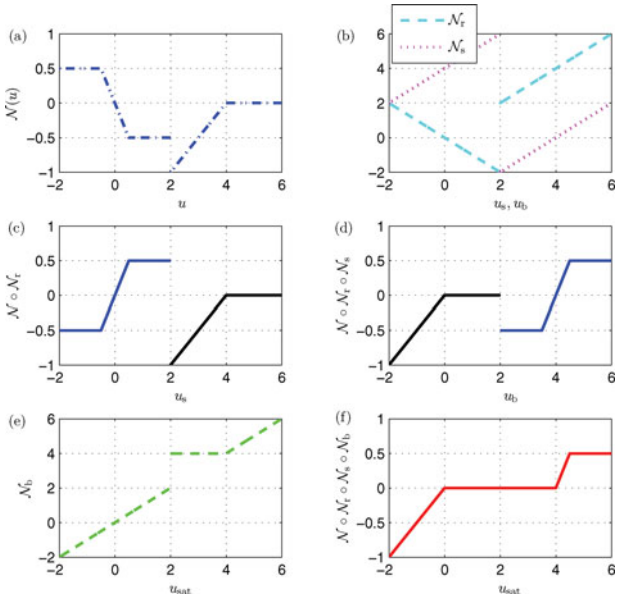

Figure 13. Example 4.14. (a) Input nonlinearity $\mathcal{N}(u)$ given by Equation (26). (b) The auxiliary reflection nonlinearity $\mathcal{N}_r$ given by Equation (27) for $u_s \in [-2, 6]$ and the auxiliary sorting nonlinearity $\mathcal{N}_s$ given by Equation (28) for $u_b \in [-2, 6]$. (c) Composite nonlinearity $\mathcal{N} \circ \mathcal{N}_r$. Note that $\mathcal{N} \circ \mathcal{N}_r$ is piecewise non-decreasing on $[-2, 6]$. (d) Composite nonlinearity $\mathcal{N} \circ \mathcal{N}_r \circ \mathcal{N}_s$. Note that $\mathcal{N} \circ \mathcal{N}_r \circ \mathcal{N}_s$ is piecewise non-decreasing on $[-2, 6]$. (e) The auxiliary blocking nonlinearity $\mathcal{N}_b$ given by Equation (29) for $u_{\rm sat} \in [-2, 6]$. (f) Composite nonlinearity $\mathcal{N} \circ \mathcal{N}_r \circ \mathcal{N}_s \circ \mathcal{N}_b$ is globally non-decreasing on $[-2, 6]$, and $\mathcal{R}_I(\mathcal{N} \circ \mathcal{N}_r \circ \mathcal{N}_s \circ \mathcal{N}_b) = \mathcal{R}_I(\mathcal{N} \circ \mathcal{N}_r \circ \mathcal{N}_b) = \mathcal{R}_I(\mathcal{N} \circ \mathcal{N}_r) = \mathcal{R}_I(\mathcal{N}) = [-1, 0.5]$.

$$\mathcal{N}_r(u_s) = \begin{cases} -u_s, & \text{if } -2 \le u_s < 2 \\ u_s, & \text{if } 2 \le u_s \le 6, \end{cases} \tag{27}$$

$$\mathcal{N}_s(u_b) = \begin{cases} u_b + 4, & \text{if } -2 \le u_b < 2 \\ u_b - 4, & \text{if } 2 \le u_b \le 6, \end{cases} \tag{28}$$

and

$$\mathcal{N}_b(u_{\rm sat}) = \begin{cases} 4, & \text{if } 2 \le u_{\rm sat} < 4 \\ u_{\rm sat}, & \text{otherwise.} \end{cases} \tag{29}$$

Figure 13(b) shows the auxiliary nonlinearities $\mathcal{N}_r$ and $\mathcal{N}_s$. Figure 13(c) and 13(d) show that the composite nonlinearity $\mathcal{N} \circ \mathcal{N}_r$ and $\mathcal{N} \circ \mathcal{N}_r \circ \mathcal{N}_s$ are piecewise non-decreasing on $I \triangleq [-2, 6]$. Figure 13(e) shows auxiliary blocking nonlinearities $\mathcal{N}_b$ and Figure 13(f) shows the composite nonlinearity $\mathcal{N} \circ \mathcal{N}_r \circ \mathcal{N}_s \circ \mathcal{N}_b$ is globally non-decreasing on I. Note that $\mathcal{R}_I(\mathcal{N} \circ \mathcal{N}_r \circ \mathcal{N}_s \circ \mathcal{N}_b) = \mathcal{R}_I(\mathcal{N} \circ \mathcal{N}_r \circ \mathcal{N}_s) = \mathcal{R}_I(\mathcal{N} \circ \mathcal{N}_r) = \mathcal{R}_I(\mathcal{N}) = [-1, 0.5]$.

Knowledge of the intervals of monotonicity of $\mathcal{N}$, the ranges of $\mathcal{N} \circ \mathcal{N}_r$ and $\mathcal{N} \circ \mathcal{N}_r \circ \mathcal{N}_s$ within each interval of monotonicity, and selected intermediate values of $\mathcal{N} \circ \mathcal{N}_r \circ \mathcal{N}_s$ in the case of partially overlapping interval ranges is needed to modify the controller output $u_{\rm sat}$ so that $\mathcal{N} \circ \mathcal{N}_r \circ \mathcal{N}_s \circ \mathcal{N}_b$ is globally non-decreasing. It thus follows that $\mathcal{N} \circ \mathcal{N}_r \circ \mathcal{N}_s \circ \mathcal{N}_b$ preserves the signs of the Markov parameters of the linearised Hammerstein system.

5. Adaptive control of Hammerstein systems with odd input nonlinearities

We now present numerical examples to illustrate the response of RCAC for Hammerstein systems with odd input nonlinearities. We consider a sequence of examples of increasing complexity, including minimum-phase and NMP plants, and asymptotically stable and unstable cases. The odd input nonlinearities may be either monotonic or non-monotonic. For each example, we assume that d and H_d are known. In all simulations, the adaptive controller gain matrix $\theta(k)$ is initialised to zero. Unless otherwise stated, all examples assume $x(0) = 0$ and $\lambda = 1$.

Example 5.1 (Minimum-phase, asymptotically stable plant, non-increasing $\mathcal{N}$): Consider the asymptotically stable, minimum-phase plant,

$$G(\mathbf{z}) = \frac{1}{\mathbf{z} - 0.5} \tag{30}$$

with the cubic input nonlinearity,

$$\mathcal{N}(u) = -u^3, \tag{31}$$

which is non-increasing, one-to-one, and onto. Note that $d = 1$ and $H_d = 1$. We consider the sinusoidal command $r(k) = 5\sin(\Omega_1 k)$, where $\Omega_1 = \pi/5$ rad/sample. Since the linear plant is minimum phase, we choose $\mathcal{N}_{\rm sat}(u_c) = {\rm sat}_{p,q}(u_c)$, where $p = -10^6$ and $q = 10^6$ in Equation (20). As shown in Figure 14(a), $\mathcal{N}$ is decreasing for all $u \in \mathbb{R}$, we let $\mathcal{N}_b = u_{\rm sat}$, $\mathcal{N}_s = u_b$, and $\mathcal{N}_r = -u_s$. Figure 14(a.iii) shows that the composite nonlinearity $\mathcal{N} \circ \mathcal{N}_r \circ \mathcal{N}_s \circ \mathcal{N}_b$ is non-decreasing. Note that knowledge of only the monotonicity of $\mathcal{N}$ is used to choose $\mathcal{N}_b$, $\mathcal{N}_s$, and $\mathcal{N}_r$. To satisfy Equation (36) in Hoagg and Bernstein (2012), a controller order nc≥5 is required. We thus let, $n_c = 10$, $P_0 = 0.01 I_{2n_c}$, $\eta_0 = 0$, and $\tilde{\mathcal{H}} = H_1$. Figure 14(b.i) and 14(b.ii) show the time history of z, while Figure 14(b.iii) shows the input nonlinearity $\mathcal{N}$ and Figure 14(b.iv) shows the time history of u. Finally, Figure 14(b.v) shows the time history of θ and Figure 14(b.vi) shows the frequency response of $G_{c,2000}(\mathbf{z})$. Note that $G_{c,2000}(\mathbf{z})$ has the form of an internal model controller with high gain at the command frequency Ω_1 and the harmonic $3\Omega_1$.

Next, the controller order n_c is increased to explore the sensitivity of the closed-loop performance to the value of n_c. For $n_c = 10, 15, 25, \ldots, 55$, the closed-loop system is simulated, where all parameters other than n_c are the same as above. The closed-loop performance in this example is insensitive to the choice of n_c provided that

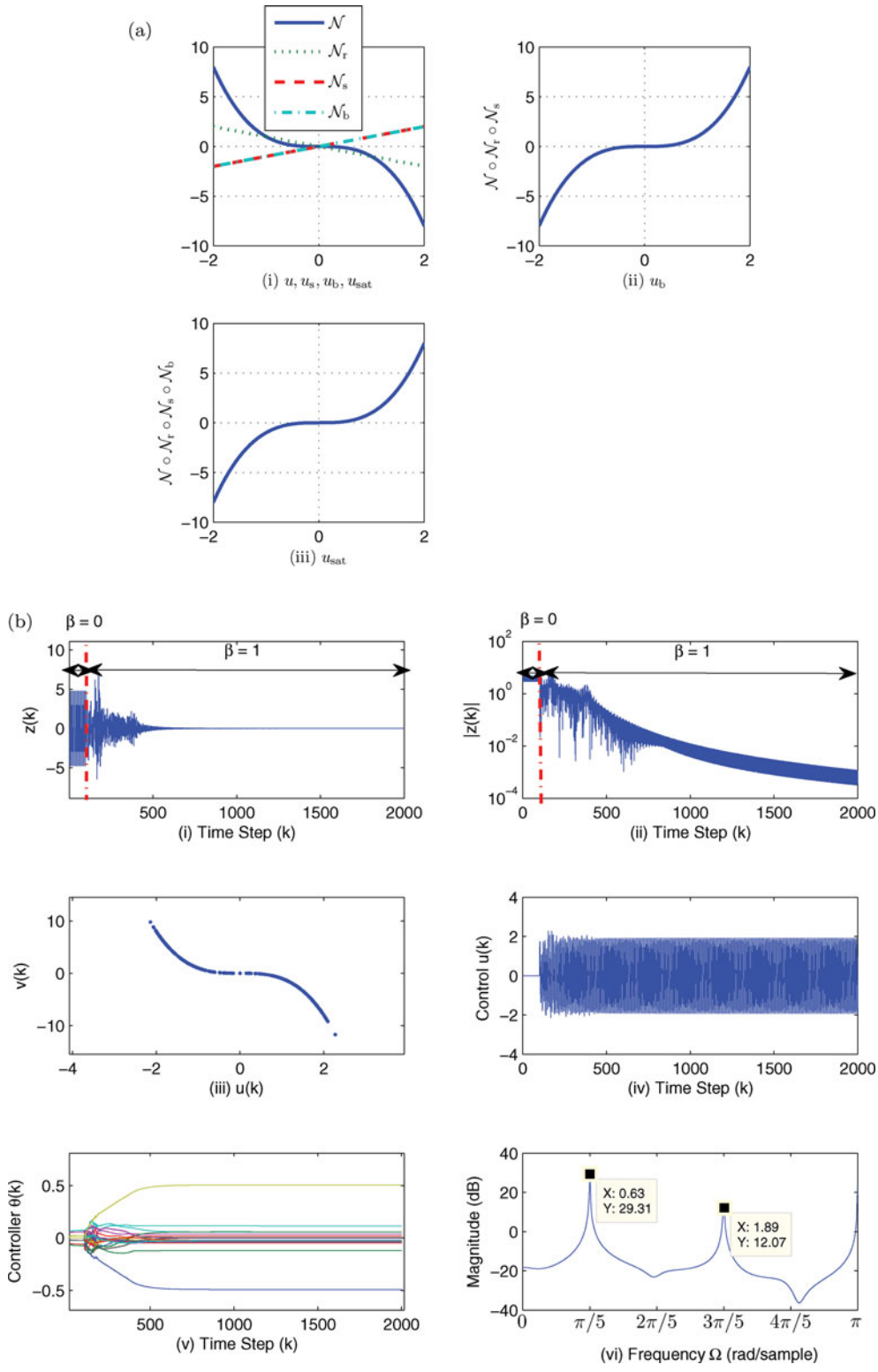

Figure 14. Example 5.1. Part (a.i) shows the nonlinear input nonlinearity $\mathcal{N}(u) = -u^3$ and the auxiliary nonlinearities $\mathcal{N}_b$, $\mathcal{N}_s$, and $\mathcal{N}_r$. (a.ii) shows the non-decreasing input nonlinearity $\mathcal{N} \circ \mathcal{N}_r \circ \mathcal{N}_s$. Part (a.iii) shows that the composite nonlinearity $\mathcal{N} \circ \mathcal{N}_r \circ \mathcal{N}_s \circ \mathcal{N}_b$ is non-decreasing. Part (b) shows the closed-loop response of the asymptotically stable minimum-phase plant G given by Equation (30) with the sinusoidal command $r(k) = 5\sin(\Omega_1 k)$, where $\Omega_1 = \pi/5$ rad/sample. Part (b.iii) shows the input nonlinearity $\mathcal{N}$ for all $u \in \mathbb{R}$, and part (b.iv) shows the time history of u. Finally, part (b.v) shows the time history of θ and part (b.vi) shows the frequency response of $G_{c,2000}(\mathbf{z})$, which indicates that $G_{c,2000}(\mathbf{z})$ has high gain at the command frequency Ω_1 and the harmonic $3\Omega_1$.

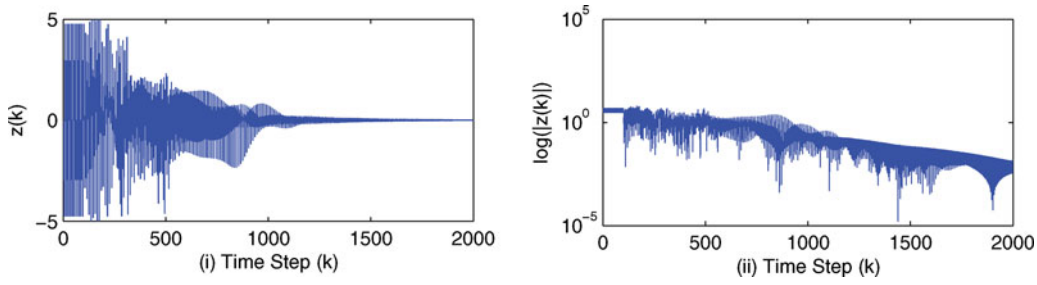

Figure 15. Example 5.1. The closed-loop response of the asymptotically stable minimum-phase plant G given by Equation (30) with the sinusoidal command $r(k) = 5\sin(\Omega_1 k)$, where $\Omega_1 = \pi/5$ rad/sample. We let $n_c = 25$, $P_0 = 0.01 I_{2n_c}$, $\eta_0 = 0$, and $\tilde{\mathcal{H}} = H_1$. The closed-loop performance is comparable to that shown in Figure 14(b).

$n_c \geq 5$, which is required to satisfy Equation (36) in Hoagg and Bernstein (2012). For this example, the worst performance is obtained by letting $n_c = 25$. Figure 15 shows the time history of z with $n_c = 25$. Over the interval of approximately $k \in [500, 1000]$, the closed-loop performance shown in Figure 15 is slightly worse than the closed-loop performance shown in Figure 14; however, the closed-loop performances are comparable over the rest of the time history.

Furthermore, consider the nonlinearity $\mathcal{N}(u) = u^n$, where n is odd, with the input signal $u(k) = \cos(\Omega k)$. Then, the response $y(k) = \mathcal{N}(u(k))$ is given by

$$y(k) = \cos^n(\Omega k) = \frac{1}{2^{n-1}} \sum_{r=0}^{(n-1)/2} \binom{n}{r} \cos[(n-2r)\Omega k]. \tag{32}$$

Note that if $\mathcal{N}$ is an odd polynomial, then $y(k)$ contains harmonics at only odd multiples of Ω. Furthermore, if $\mathcal{N}$ is an odd analytic function such as $\mathcal{N}(u) = \sin u$, then this observation applies to truncations of its Taylor expansion.

Example 5.2 (NMP, asymptotically stable plant, non-decreasing $\mathcal{N}$): We consider the asymptotically stable, NMP plant,

$$G(\mathbf{z}) = \frac{\mathbf{z} - 1.5}{(\mathbf{z} - 0.8)(\mathbf{z} - 0.6)} \tag{33}$$

with the saturation input nonlinearity,

$$\mathcal{N}(u) = \begin{cases} -0.8, & \text{if } u < -0.8 \\ u, & \text{if } -0.8 \leq u \leq 0.8 \\ 0.8, & \text{if } u > 0.8, \end{cases} \tag{34}$$

which is non-decreasing and one-to-one but not onto. Note that $d = 1$ and $H_d = 1$. We consider the two-tone sinusoidal command $r(k) = 0.5\sin(\Omega_1 k) + 0.5\sin(\Omega_2 k)$, where $\Omega_1 = \pi/5$ rad/sample and $\Omega_2 = \pi/2$ rad/sample for the Hammerstein system with the input nonlinearity $\mathcal{N}$. As shown in Figure 16(a), since $\mathcal{N}$ is non-decreasing for all $u \in \mathbb{R}$, we choose $\mathcal{N}_{\text{sat}}(u_c) = \text{sat}_{p,q}(u_c)$, where $p = -2$ and $q = 2$ in Equation (20), and let $\mathcal{N}_b = u_{\text{sat}}$, $\mathcal{N}_s = u_b$, and $\mathcal{N}_r = u_s$. Figure 16(a.iii) shows that the composite nonlinearity $\mathcal{N} \circ \mathcal{N}_r \circ \mathcal{N}_s \circ \mathcal{N}_b$ is non-decreasing on $[-2, 2]$. We set $n_c = 10$, $P_0 = 0.1 I_{2n_c}$, $\eta_0 = 2$, and $\tilde{\mathcal{H}} = H_1$. The Hammerstein system runs open loop for 100 time steps, and RCAC is turned on at $k = 100$. Figure 16(b) shows the time history of z. Figure 16(c) shows the frequency response of $G_{c,1000}(\mathbf{z})$, which indicates that $G_{c,1000}(\mathbf{z})$ has high gain at the command frequencies Ω_1 and Ω_2.

Example 5.3 (NMP, asymptotically stable plant, non-decreasing $\mathcal{N}$): To illustrate the choice of $\mathcal{N}_{\text{sat}}$ for an NMP plant, consider Equation (33) with the dead-zone input nonlinearity:

$$\mathcal{N}(u) = \begin{cases} u + 0.5, & \text{if } u < -0.5 \\ 0, & \text{if } -0.5 \leq u \leq 0.5 \\ u - 0.5, & \text{if } u > 0.5, \end{cases} \tag{35}$$

which is not one-to-one but onto. Note that $d = 1$ and $H_d = 1$. We consider the two-tone sinusoidal command $r(k) = \sin(\Omega_1 k) + 0.5\sin(\Omega_2 k)$, where $\Omega_1 = \pi/4$ rad/sample, and $\Omega_2 = \pi/2$ rad/sample. As shown in Figure 17(a), since $\mathcal{N}(u)$ is non-decreasing for all $u \in \mathbb{R}$, we choose $\mathcal{N}_{\text{sat}}(u_c) = \text{sat}_{p,q}(u_c)$, where $p = -a$, $q = a$, and let $\mathcal{N}_b = u_{\text{sat}}$, $\mathcal{N}_s = u_b$, and $\mathcal{N}_r = u_s$ on $\mathbb{R}$. Figure 17(a.iii) shows that the composite nonlinearity $\mathcal{N} \circ \mathcal{N}_r \circ \mathcal{N}_s \circ \mathcal{N}_b$ is non-decreasing on $\mathbb{R}$. We set $n_c = 10$, $P_0 = 0.1 I_{2n_c}$, $\eta_0 = 0.2$, and $\tilde{\mathcal{H}} = H_1$, and we vary the saturation level a for the NMP plant (33). Figure 17(b.i) shows the time history of z with $a = 10$, where the transient behaviour is poor. Figure 17(b.ii) shows the time history of z with $a = 2$, where the transient performance is improved and z reaches steady state in about 300 time steps. Finally, we further reduce the saturation level. Figure 17(b.iii) shows the time history of z with $a = 1$; in this case, RCAC cannot follow the command due to the fact that $a = 1$ is not large enough to provide the control u_c needed to drive z to a small value. Figure 17(c) shows the time history of u for the case $a = 2$, and Figure 17(d) shows the frequency response of $G_{c,1200}(\mathbf{z})$ with $a = 2$, which indicates that $G_{c,1200}(\mathbf{z})$ has high gain at the command frequencies Ω_1 and Ω_2.

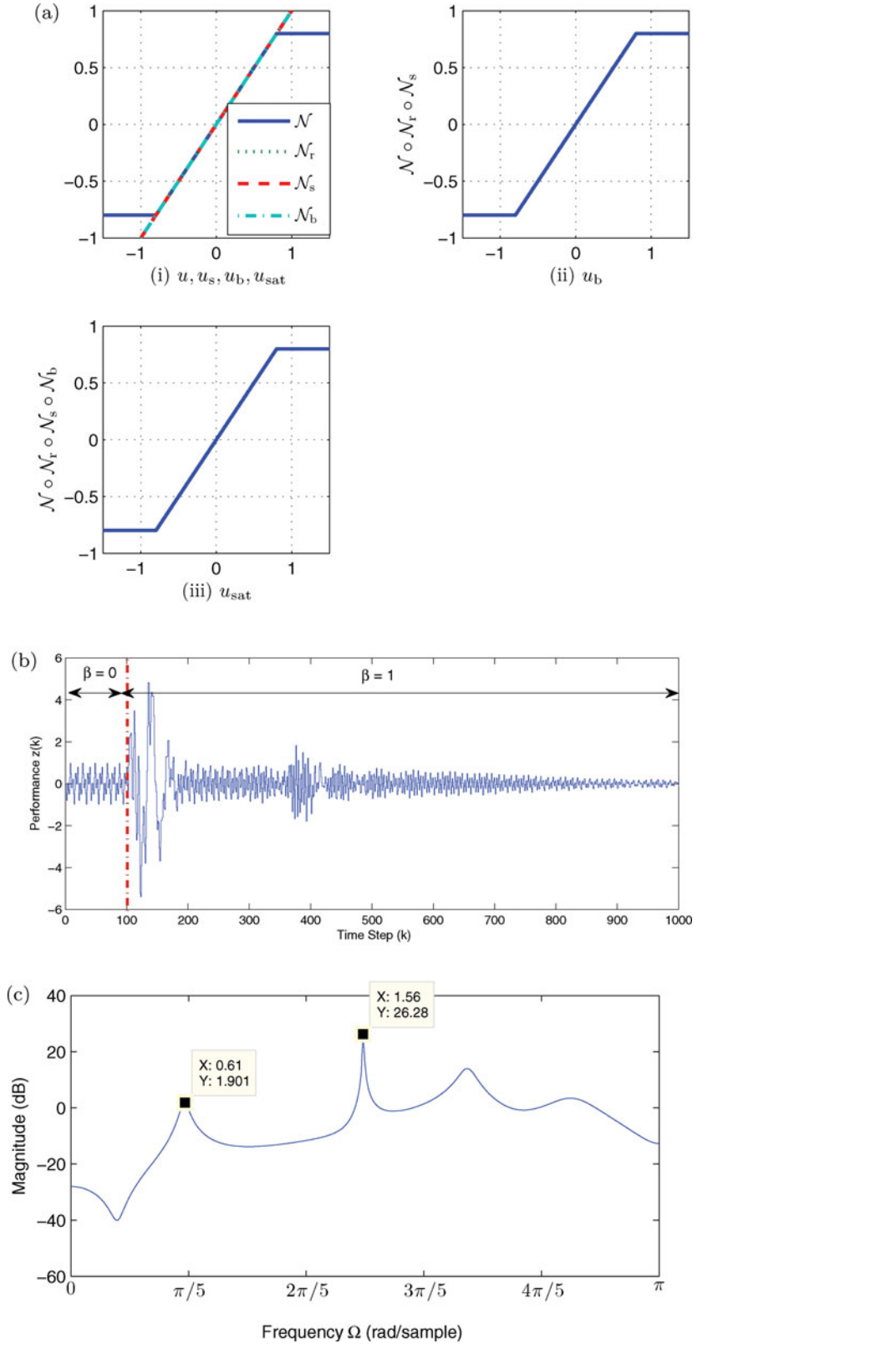

Figure 16. Example 5.2. Part (a) shows the saturation input nonlinearity $\mathcal{N}$ given by Equation (34). Part (b) shows the closed-loop response of the asymptotically stable NMP plant G given by Equation (33) with the two-tone sinusoidal command $r(k) = 0.5\sin(\Omega_1 k) + 0.5\sin(\Omega_2 k)$, $\Omega_1 = \pi/5$ rad/sample, and $\Omega_2 = \pi/2$ rad/sample. Part (c) shows the frequency response of $G_{c,1000}(\mathbf{z})$, which indicates that $G_{c,1000}(\mathbf{z})$ has high gain at the command frequencies Ω_1 and Ω_2.

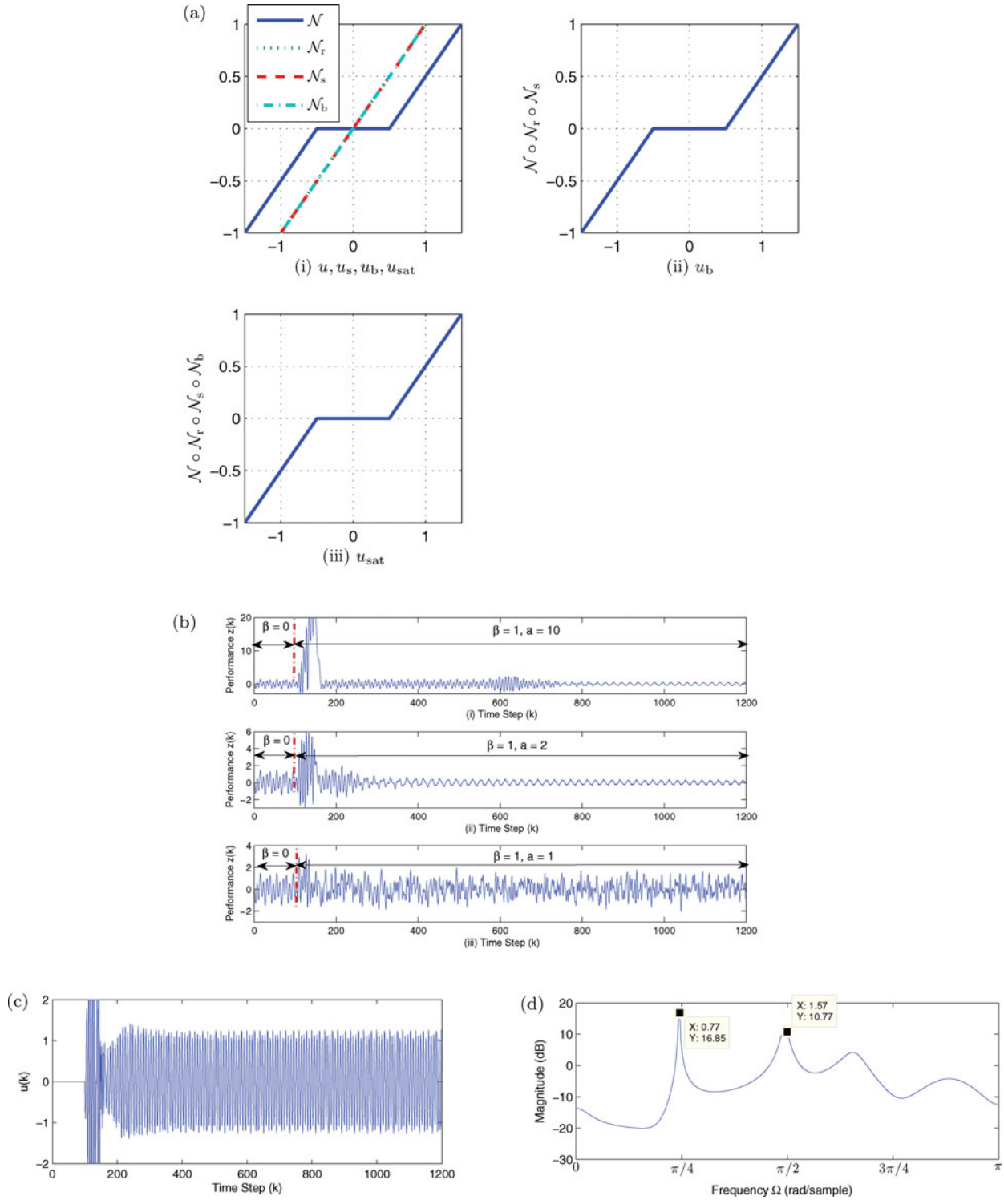

Figure 17. Example 5.3. Part (a) shows the dead-zone input nonlinearity $\mathcal{N}(u)$ given by Equation (35). Part (b) shows the closed-loop response of the asymptotically stable NMP plant G given by Equation (33) with the two-tone sinusoidal command $r(k) = \sin(\Omega_1 k) + 0.5\sin(\Omega_2 k)$, where $\Omega_1 = \pi/4$ rad/sample and $\Omega_2 = \pi/10$ rad/sample. Part (b.i) shows the time history of the performance z with $a = 10$, where the transient behaviour is poor. Part (b.ii) shows the time history of z with $a = 2$. Note that the transient performance is improved and z reaches steady state in about 300 time steps. Finally, part (b.iii) shows the time history of z with $a = 1$; in this case, RCAC cannot follow the command due to the fact that $a = 1$ is not large enough to provide the control u_c needed to drive z to a small value. Part (c) shows the time history of u for the case $a = 2$, and part (d) shows the frequency response of $G_{c,1200}(\mathbf{z})$ with $a = 2$, which indicates that $G_{c,1200}(\mathbf{z})$ has high gain at the command frequencies Ω_1 and Ω_2.

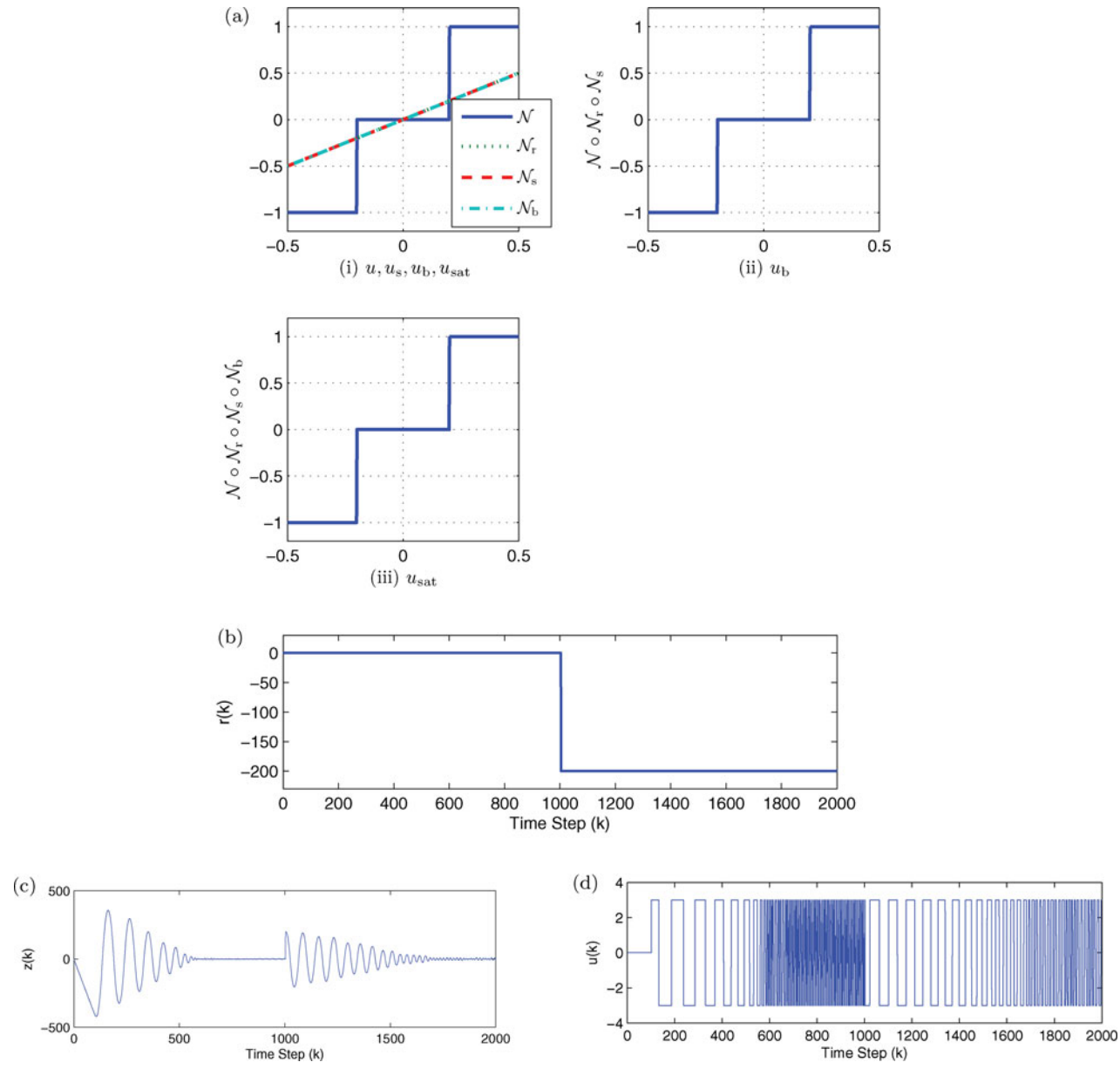

Figure 18. Example 5.4. Closed-loop response of the plant G given by Equation (36) with the initial condition $x_0 = [-5.2 \ -1.1]^T$. The system runs open loop for 100 time steps, and the adaptive controller is turned on at $k = 100$ with the relay input nonlinearity given by Equation (37) and $x(100) = [-415.2 \ -411.1]^T$. For $k \geq 1000$, the command is the step $r(k) = -200$ as shown in (b). Part (c) shows the time history of the performance z, and part (d) shows the time history of u.

Example 5.4 (Minimum-phase, unstable plant, non-decreasing $\mathcal{N}$): We consider the discretised unstable double-integrator plant over sample period $h = 1/\sqrt{2}$,

$$G(\mathbf{z}) = \frac{h^2(\mathbf{z}+1)}{2(\mathbf{z}-1)^2} \tag{36}$$

with the piecewise-constant input nonlinearity,

$$\mathcal{N}(u) = \frac{1}{2}[\text{sign}(u-0.2) + \text{sign}(u+0.2)], \tag{37}$$

which can assume only the values -1, 0, and 1. Note that $d = 1$ and $H_d = 1$. For $k < 1000$, we let the command $r(k)$ be zero, and consider stabilisation using RCAC with the input relay nonlinearity given by Equation (37). As shown in Figure 18(a), the relay nonlinearity is non-decreasing for all $u \in \mathbb{R}$, and we thus choose $\mathcal{N}_{\text{sat}}(u_c) = \text{sat}_{p,q}(u_c)$, where $p = -3$, $q = 3$. We let $\mathcal{N}_b = u_{\text{sat}}$, $\mathcal{N}_s = u_b$, and $\mathcal{N}_r = u_s$. We choose $n_c = 2$, $P_0 = I_{2n_c}$, $\eta_0 = 0$, and $\tilde{\mathcal{H}} = H_1$. For $k \geq 1000$, we let the step command be $r(k) = -200$, and consider command-following problem as shown in Figure 18(b).

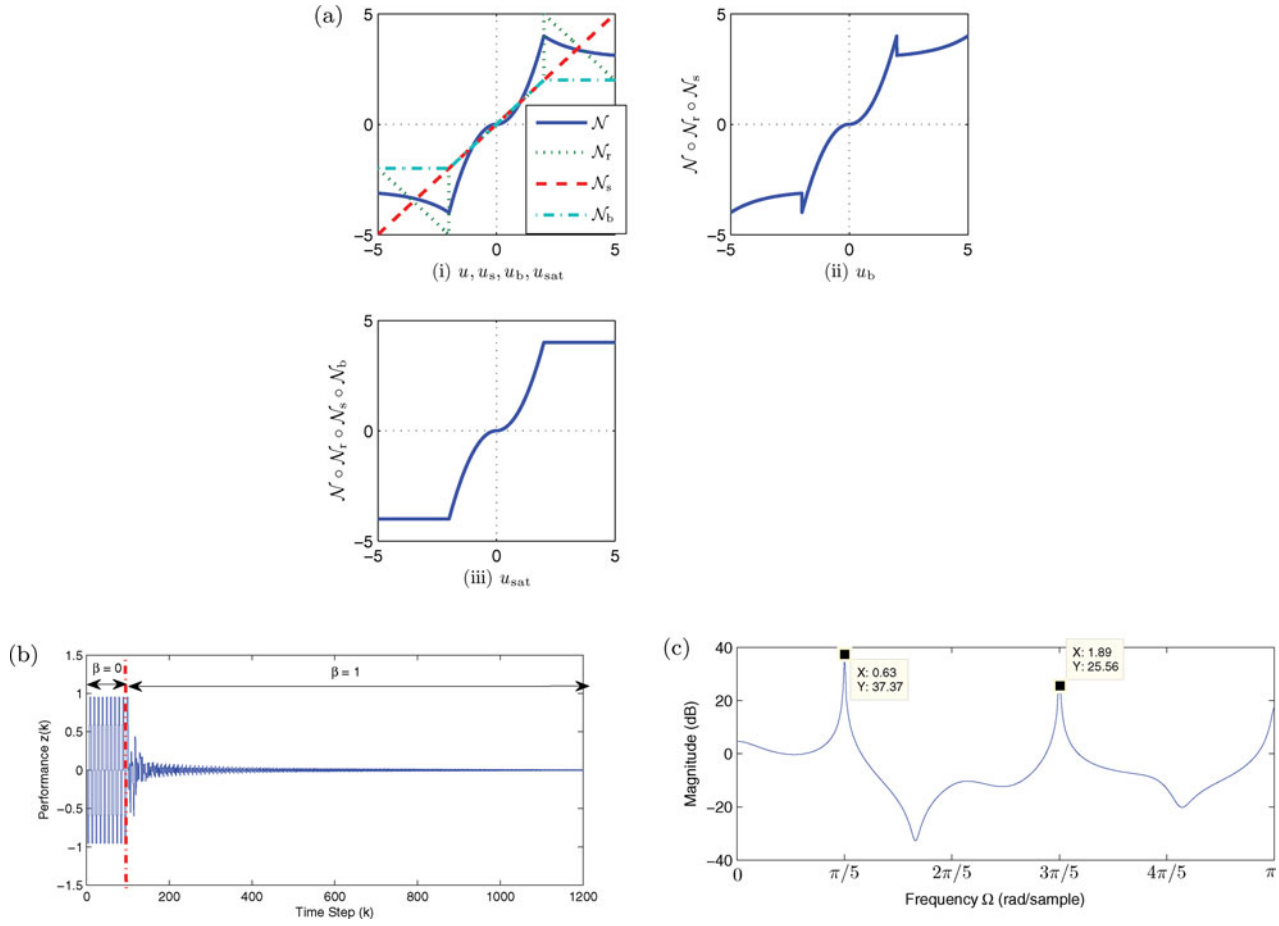

Figure 19. Example 5.5. Part (a.i) shows the input nonlinearity (39) and the auxiliary nonlinearities $\mathcal{N}_b$ and $\mathcal{N}_r$. Part (a.ii) shows the piecewise non-decreasing input nonlinearity $\mathcal{N} \circ \mathcal{N}_r$. Part (a.iii) shows that the composite nonlinearity $\mathcal{N} \circ \mathcal{N}_r \circ \mathcal{N}_b$ is nondecreasing. Part (b) shows the closed-loop response of the stable minimum-phase plant G given by Equation (38) with the sinusoidal command $r(k) = \sin(\Omega_1 k)$, where $\Omega_1 = \pi/5$ rad/sample. Part (c) shows the frequency response of $G_{c,1200}(\mathbf{z})$, which indicates that $G_{c,1200}(\mathbf{z})$ has high gain at the command frequency Ω_1 and the harmonic $3\Omega_1$.

Figure 18(c) shows the time history of z with the initial condition $x_0 = [-5.2 \ \ -1.1]^T$ and (d) shows the time history of u.

Example 5.5 (Minimum-phase, asymptotically stable plant, non-monotonic $\mathcal{N}$): Consider the asymptotically stable,minimum-phase plant,

$$G(\mathbf{z}) = \frac{(\mathbf{z} - 0.5)(\mathbf{z} - 0.9)}{(\mathbf{z} - 0.7)(\mathbf{z} - 0.5 - \jmath 0.5)(\mathbf{z} - 0.5 + \jmath 0.5)} \quad (38)$$

with the non-monotonic input nonlinearity,

$$\mathcal{N}(u) = \begin{cases} -0.5^{-(u+2)} - 3, & \text{if } u < -2 \\ \text{sign}(u)u^2, & \text{if } -2 \le u \le 2 \\ 0.5^{u-2} + 3, & \text{if } u > 2. \end{cases} \quad (39)$$

Note that $d = 1$ and $H_d = 1$. We consider the sinusoidal command $r(k) = \sin(\Omega_1 k)$, where $\Omega_1 = \pi/5$ rad/sample. Since the linear plant is minimum phase, we choose $\mathcal{N}_{\text{sat}}(u_c) = \text{sat}_{p,q}(u_c)$, where $p = -5$ and $q = 5$ in (20). As shown in Figure 19(a.i), $\mathcal{N}$ is non-monotonic, we let $\mathcal{N}_r(u_s) = -u_s - 7$ for $u_s \in [-5, -2]$, $\mathcal{N}_r(u_s) = -u_s + 7$ for $u_s \in [2, 5]$, and $\mathcal{N}_r(u_s) = u_s$ otherwise, and choose $N_s(u_b) = u_b$ so that the composite nonlinearity $\mathcal{N} \circ \mathcal{N}_r \circ \mathcal{N}_s$ is piecewise non-decreasing on $[-5, 5]$ as shown in Figure 19(a.ii). Knowledge of only the monotonicity of $\mathcal{N}$ is used to choose $\mathcal{N}_r$. To construct $\mathcal{N}_b$, note that the piecewise non-decreasing composite nonlinearity $\mathcal{N} \circ \mathcal{N}_r \circ \mathcal{N}_s$ satisfies $\mathcal{R}_{[-5,-2]}(\mathcal{N} \circ \mathcal{N}_r \circ \mathcal{N}_s) \cup \mathcal{R}_{[2,5]}(\mathcal{N} \circ \mathcal{N}_r \circ \mathcal{N}_s) \subset \mathcal{R}_{[-5,5]}(\mathcal{N} \circ \mathcal{N}_r \circ \mathcal{N}_s)$, which is not partially overlapping. Therefore, no additional information about $\mathcal{N} \circ \mathcal{N}_r \circ \mathcal{N}_s$ is needed. We let $\mathcal{N}_b(u_{\text{sat}}) = -2$ for $u_{\text{sat}} \in [-5, -2]$, $\mathcal{N}_b(u_{\text{sat}}) = 2$ for $u_{\text{sat}} \in [2, 5]$ and $\mathcal{N}_b(u_{\text{sat}}) = u_{\text{sat}}$ otherwise. Figure 19(a.iii) shows that the composite nonlinearity $\mathcal{N} \circ \mathcal{N}_r \circ \mathcal{N}_s \circ \mathcal{N}_b$ is non-decreasing on $[-5, 5]$. We choose $n_c = 10$, $P_0 = I_{2n_c}$, $\eta_0 = 0.01$, and $\tilde{\mathcal{H}} = H_1$. Figure 19(b) shows the resulting time history of z, while Figure 19(c) shows the frequency response of $G_{c,1200}(\mathbf{z})$ with $a = 2$. Note that $G_{c,1200}(\mathbf{z})$ has high gain at the command frequency Ω_1 and the harmonic $3\Omega_1$.

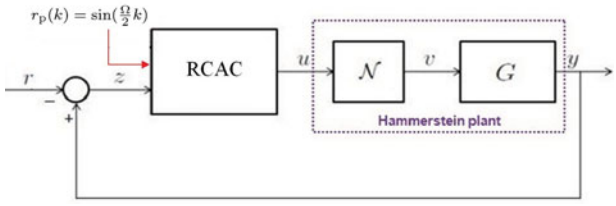

Figure 20. Adaptive command-following problem for a Hammerstein plant with an even input nonlinearity $\mathcal{N}$. The command signal r has frequency Ω and phase angle ϕ, while the pseudo-command is a sinusoid with frequency $\Omega/2$. The pseudo-command provides the harmonic content needed by RCAC due to the even nonlinearity, which produces harmonics at only DC and 2Ω.

6. Adaptive control of Hammerstein systems with even input nonlinearities

We now present numerical examples to illustrate the response of RCAC for Hammerstein systems with even input nonlinearities. Consider the nonlinearity $\mathcal{N}(u) = u^n$, where n is even, with the input signal $u(k) = \cos(\Omega k)$. Then the response $y(k) = \mathcal{N}(u(k))$ is given by

$$y(k) = \cos^n(\Omega k) = \frac{1}{2^n}\binom{n}{n/2} + \frac{1}{2^{n-1}}\sum_{r=0}^{n/2-1}\binom{n}{r}\cos((n-2r)\Omega k). \quad (40)$$

Therefore, if $\mathcal{N}$ is an even polynomial, then $y(k)$ contains harmonics at only even multiples of Ω. In particular, $y(k)$ lacks spectral content at the command frequency. If $\mathcal{N}$ is an even analytic function, then this observation applies to truncations of its Taylor expansion.

To achieve command following in this case, we propose two approaches. First, we inject a pseudo-command into the controller, where the frequency of the pseudo-command is equal to half of the frequency of the command as shown in Figure 20. Therefore, the plant intermediate signal v contains a harmonic at the command frequency Ω if $\mathcal{N}$ is even. Note that the pseudo-command is not necessarily phase matched with the command. Alternatively, we use auxiliary nonlinearities to construct a composite input nonlinearities that is not even.

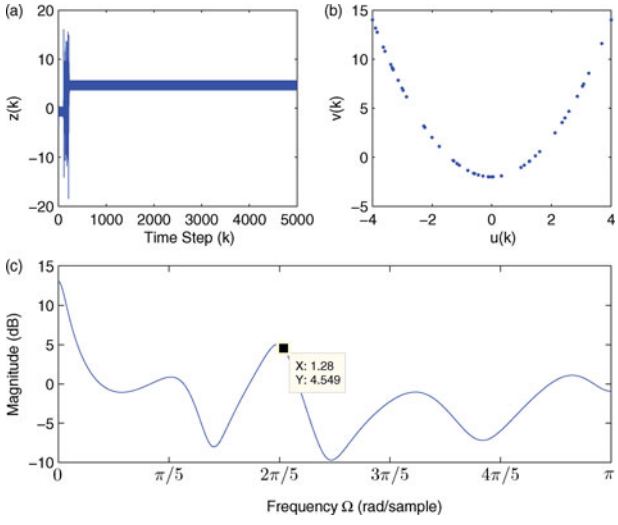

Figure 21. Example 6.1. Part (a) shows the resulting time history of the command-following performance z. In this case, the adaptive controller fails to follow the command in the presence of the quadratic input nonlinearity (41). Part (c) shows the frequency response of $G_{c,5000}(\mathbf{z})$, which indicates that $G_{c,5000}(\mathbf{z})$ has high gain at $2\Omega_1 = 2\pi/5$ rad/sample, but not at the command frequency $\Omega_1 = \pi/5$ rad/sample.

6.1 Adaptive control of Hammerstein systems with even input nonlinearities using pseudo-commands

Example 6.1 (Minimum-phase, stable plant, even $\mathcal{N}$): We consider the asymptotically stable, NMP plant (38) with the quadratic input nonlinearity:

$$\mathcal{N}(u) = u^2 - 2, \quad (41)$$

which is neither one-to-one nor onto and satisfies $\mathcal{N}(0) = -2$, see Figure 21(b). Note that $d = 1$ and $H_d = 1$. We

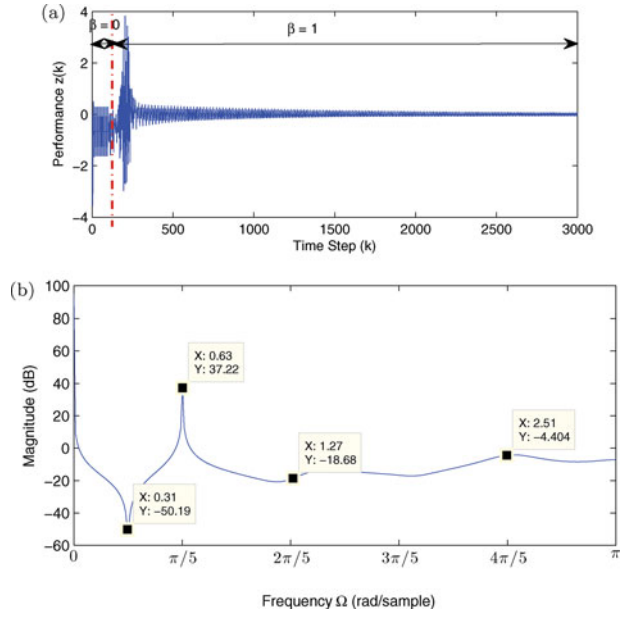

Figure 22. Example 6.2. Adaptive command-following problem for a Hammerstein plant with an even input nonlinearity (41). The command signal $r(k) = \sin(\Omega_1 k + \phi)$, where $\Omega_1 = \pi/5$ rad/sample and $\phi = \pi/6$ rad. The Hammerstein system runs open loop for 100 time steps, and RCAC with the pseudo-command $r_p(k) = \sin(\frac{\Omega_1}{2}k)$ is turned on at $k = 100$. Part (a) shows the time history of z. Part (b) shows the frequency response of $G_{c,3000}(\mathbf{z})$, which indicates that $G_{c,3000}(\mathbf{z})$ has high gain at the command frequency $\Omega_1 = \pi/5$ rad/sample.

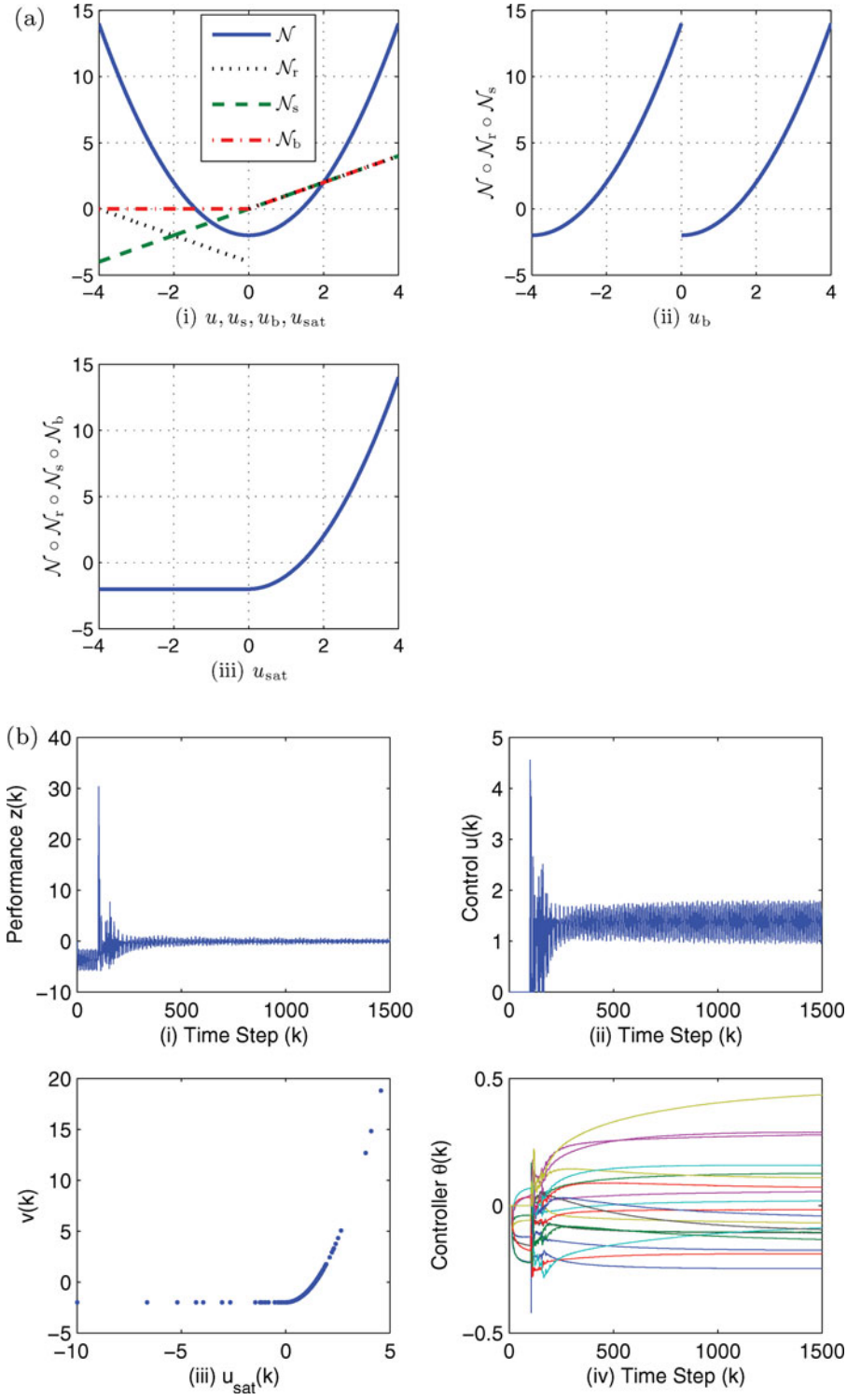

Figure 23. Example 6.3. Part (a.i) shows the quadratic input nonlinearity $\mathcal{N}(u) = u^2 - 2$ and the auxiliary nonlinearities $\mathcal{N}_b$ and $\mathcal{N}_r$. Part (a.ii) shows the piecewise non-decreasing input nonlinearity $\mathcal{R}_{[-4,0)}(\mathcal{N} \circ \mathcal{N}_r \circ \mathcal{N}_s) \subset \mathcal{R}_{[0,4]}(\mathcal{N} \circ \mathcal{N}_r \circ \mathcal{N}_s)$, which is not partially overlapping. Part (a.iii) shows that the composite nonlinearity $\mathcal{N} \circ \mathcal{N}_r \circ \mathcal{N}_s \circ \mathcal{N}_b$ is non-decreasing. Part (b) shows the closed-loop response of the stable minimum-phase plant G given by Equation (30) with the sinusoidal command $r(k) = \sin(0.2\pi k)$ and disturbance $w(k) = 0.5 \sin(\frac{\pi}{2}k)$.

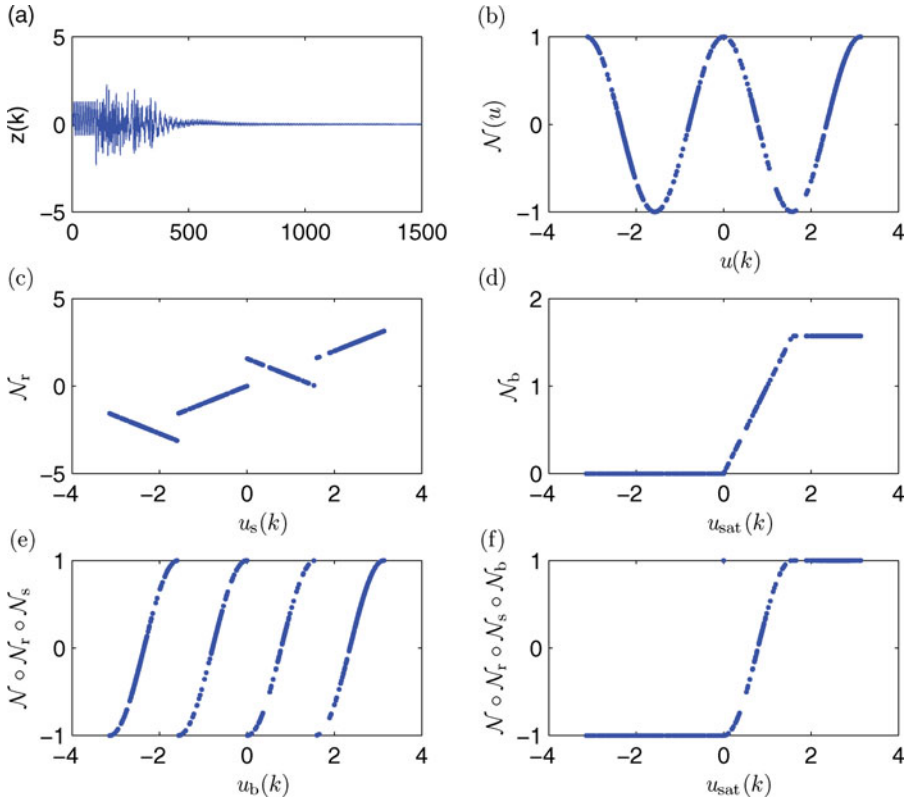

Figure 24. Example 6.4. Part (a) shows that RCAC follows the sinusoidal command for the Hammerstein system. Part (b) shows the input nonlinearity $\mathcal{N}$, parts (c) and (d) show the auxiliary nonlinearities $\mathcal{N}_r$ and $\mathcal{N}_b$, part (e) shows that the composite nonlinearity $\mathcal{N} \circ \mathcal{N}_r \circ \mathcal{N}_s$ is piecewise increasing, and part (f) shows that the composite nonlinearity $\mathcal{N} \circ \mathcal{N}_r \circ \mathcal{N}_s \circ \mathcal{N}_b$ is non-decreasing.

consider the sinusoidal command $r(k) = \sin(\Omega_1 k)$, where $\Omega_1 = \pi/5$ rad/sample. We let $n_c = 10$, $P_0 = I_{2n_c}$, $\eta_0 = 0.01$, $\tilde{\mathcal{H}} = H_1$, and do not use a pseudo-command. Figure 21(a) shows the resulting time history of z. In this case, the adaptive controller fails to follow the command in the presence of the input nonlinearity. Figure 21(c) shows the frequency response of $G_{c,5000}(\mathbf{z})$, which has high gain at $2\Omega_1$, but not at the command frequency Ω_1.

Example 6.2 (Minimum-phase, stable plant, even $\mathcal{N}$, and pseudo-command): As in Example 6.1, we consider the asymptotically stable, NMP plant (38) with the quadratic input nonlinearity (41) and the sinusoidal command $r(k) = \sin(\Omega_1 k + \phi)$, where $\Omega_1 = \pi/5$ rad/sample and $\phi = \pi/6$ rad. The pseudo-command frequency is $\Omega_p = \Omega_1/2 = \pi/10$ rad/sample, and we let $n_c = 10$, $P_0 = 0.01 I_{2n_c}$, $\eta_0 = 0.01$, and $\tilde{\mathcal{H}} = H_1$. The Hammerstein system runs open loop for 100 time steps, and RCAC is turned on at $k = 100$. Figure 22(a) shows the time history of z. Figure 22(b) shows the frequency response of $G_{c,3000}(\mathbf{z})$, which has high gain at the command frequency Ω_1.

6.2 *Adaptive control of Hammerstein systems with even input nonlinearities using auxiliary nonlinearities*

We now present numerical examples for RCAC controller with auxiliary nonlinearities under the condition that the input nonlinearity is even. The auxiliary nonlinearities are used such that the input nonlinearity $\mathcal{N} \circ \mathcal{N}_r \circ \mathcal{N}_s \circ \mathcal{N}_b$ is globally non-decreasing and thus not even.

Example 6.3: We consider the asymptotically stable, NMP plant,

$$G(\mathbf{z}) = \frac{\mathbf{z} - 1.2}{\mathbf{z}^2 + 0.3\mathbf{z} - 0.1}, \tag{42}$$

with the quadratic input nonlinearity (41), which is neither one-to-one nor onto and satisfies $\mathcal{N}(0) = -2$. Note that $d = 1$ and $H_d = 1$. As shown in Figure 23(a.i), since $\mathcal{N}(u)$ is not monotonic and G is NMP, we choose $\mathcal{N}_{sat}(u_c) = \text{sat}_{p,q}(u_c)$, where $p = -4$ and $q = 4$ in Equation (20), let $\mathcal{N}_r(u_b) = -u_b - 4$ for $u_b \in [-4, 0]$ and $\mathcal{N}_r(u_b) = u_b$ otherwise, and select $\mathcal{N}_s(u_b) = u_b$ so that the composite nonlinearity $\mathcal{N} \circ \mathcal{N}_r \circ \mathcal{N}_s$ is piecewise non-decreasing in Figure 23(a.ii).

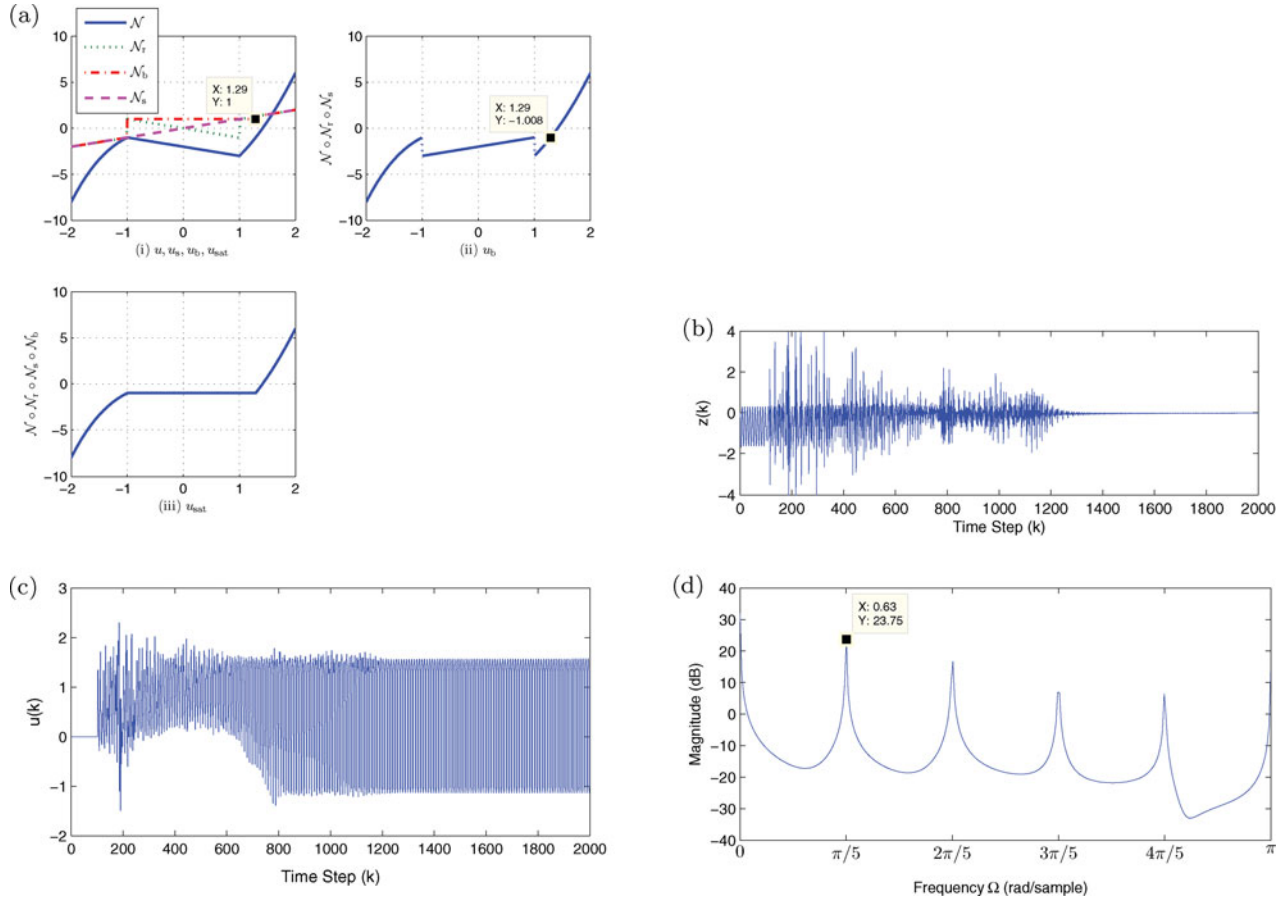

Figure 25. Example 7.1. Part (a.i) shows the input nonlinearity $\mathcal{N}(u)$ given by Equation (45) and the auxiliary nonlinearities $\mathcal{N}_b$ and $\mathcal{N}_r$. Part (a.ii) shows the piecewise non-decreasing input nonlinearity $\mathcal{N} \circ \mathcal{N}_r \circ \mathcal{N}_s$ with partially overlapping intervals. Part (a.iii) shows that the composite nonlinearity $\mathcal{N} \circ \mathcal{N}_r \circ \mathcal{N}_s \circ \mathcal{N}_b$ is non-decreasing. Part (b) shows the closed-loop response to the sinusoidal command $r(k) = \sin(0.2\pi k)$ of the stable minimum-phase plant G given by Equation (44). Part (b) shows the resulting time history of z, and part (c) shows the time history of u. Finally, part (d) shows the frequency response of $G_{c,2000}(\mathbf{z})$, which indicates that $G_{c,2000}(\mathbf{z})$ has high gain at the command frequency $\Omega = \pi/5$ rad/sample.

Knowledge of only the monotonicity of $\mathcal{N}$ is used to choose $\mathcal{N}_r$. To construct $\mathcal{N}_b$, note that the piecewise non-decreasing composite nonlinearity $\mathcal{N} \circ \mathcal{N}_r \circ \mathcal{N}_s$ satisfies $\mathcal{R}_{[-4,0)}(\mathcal{N} \circ \mathcal{N}_r \circ \mathcal{N}_s) \subset \mathcal{R}_{[0,4]}(\mathcal{N} \circ \mathcal{N}_r \circ \mathcal{N}_s)$, which is not partially overlapping. Therefore, no additional information about $\mathcal{N} \circ \mathcal{N}_r \circ \mathcal{N}_s$ is needed. We let $\mathcal{N}_b(u_{\rm sat}) = 0$ for $u_{\rm sat} \in [-4, 0)$ and $\mathcal{N}_b(u_{\rm sat}) = u_{\rm sat}$ otherwise. Figure 23(a.iii) shows that the composite nonlinearity $\mathcal{N} \circ \mathcal{N}_r \circ \mathcal{N}_s \circ \mathcal{N}_b$ is non-decreasing.

We consider the single-tone sinusoidal command $r(k) = \sin \Omega_1 k$, where $\Omega_1 = \pi/5$ rad/sample, and the disturbance $w(k) = 0.5 \sin(\frac{\pi}{2}k)$. We let $n_c = 10$, $P_0 = 0.01 I_{2n_c}$, $\eta_0 = 0.1$, and $\tilde{\mathcal{H}} = H_1$. Figure 23(b) shows the time history of z with the input nonlinearity and disturbance present and RCAC is able to follow the command.

Example 6.4: We consider the asymptotically stable, minimum-phase plant (30) with the non-monotonic input nonlinearity:

$$\mathcal{N}(u) = \cos(2u), \tag{43}$$

which is neither one-to-one nor onto and satisfies $\mathcal{N}(0) = 1$. Note that $d = 1$ and $H_d = 1$. As shown in Figure 24(b), $\mathcal{N}(u)$ is increasing for all $u \in \bigcup_{n\in\mathbb{Z}} \left((n - \frac{1}{2})\pi, n\pi\right)$, and decreasing for all $u \in \bigcup_{n\in\mathbb{Z}} \left(n\pi, (n + \frac{1}{2})\pi\right)$. We thus choose $\mathcal{N}_{\rm sat}(u_c) = {\rm sat}_{p,q}(u_c)$, where $p = -10^6$ and $q = 10^6$ in Equation (20), let $\mathcal{N}_r(u_s) = u_s$ in the intervals where $\mathcal{N}$ is increasing, and $\mathcal{N}_r(u_s) = -u_s + (2n + 1/2)\pi$ in the intervals where $\mathcal{N}$ is decreasing, and select $\mathcal{N}_s(u_b) = u_b$. The composite nonlinearity $\mathcal{N} \circ \mathcal{N}_r \circ \mathcal{N}_s$ is piecewise non-decreasing in Figure 24(e). Knowledge of only the monotonicity intervals of $\mathcal{N}$ is used to choose $\mathcal{N}_r$. To construct $\mathcal{N}_b$, note that the piecewise non-decreasing composite nonlinearity $\mathcal{N} \circ \mathcal{N}_r \circ \mathcal{N}_s$ satisfies $\mathcal{R}_{I_i}(\mathcal{N} \circ \mathcal{N}_r \circ \mathcal{N}_s) \subset \mathcal{R}_{I_j}(\mathcal{N} \circ \mathcal{N}_r \circ \mathcal{N}_s)$ for all $i \neq j$. Therefore, no

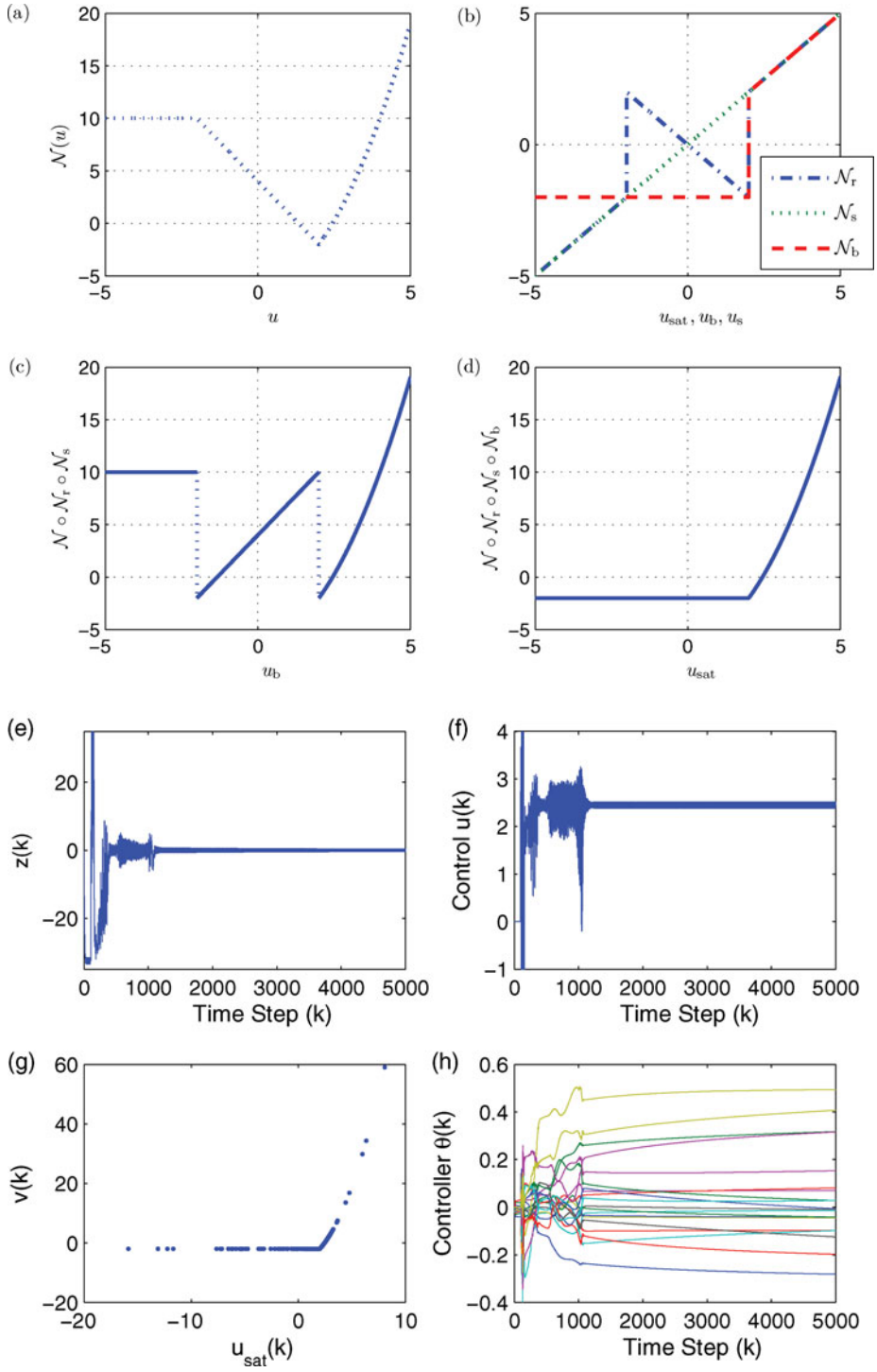

Figure 26. Example 7.2. Part (a) shows the non-monotonic input nonlinearity $\mathcal{N}(u)$ given by Equation (22), and part (b) shows the auxiliary nonlinearities $\mathcal{N}_b$ and $\mathcal{N}_r$. Part (c) shows that the composite nonlinearity $\mathcal{N} \circ \mathcal{N}_r \circ \mathcal{N}_s$ is piece-wise non-decreasing. Part (d) shows that the composite nonlinearity $\mathcal{N} \circ \mathcal{N}_r \circ \mathcal{N}_s \circ \mathcal{N}_b$ is globally non-decreasing. Part (e) shows the closed-loop response to the sinusoidal command $r(k) = \sin(0.2\pi k)$ of the stable minimum-phase plant G given by Equation (46). Part (f) shows the resulting time history of u, and (h) shows the time history of θ.

additional information of $\mathcal{N} \circ \mathcal{N}_r \circ \mathcal{N}_s$ is needed. We let $\mathcal{N}_b(u_{\rm sat}) = 0$ for $u_{\rm sat} < 0$, $\mathcal{N}_b(u_{\rm sat}) = \pi/2$ for $u_{\rm sat} > \pi/2$ and $\mathcal{N}_b(u_{\rm sat}) = u_{\rm sat}$ otherwise. Figure 24(f) shows that the composite nonlinearity $\mathcal{N} \circ \mathcal{N}_r \circ \mathcal{N}_s \circ \mathcal{N}_b$ is non-decreasing.

We consider the single-tone sinusoidal command $r(k) = \sin \Omega_1 k$, where $\Omega_1 = \pi/5$ rad/sample. We let $n_{\rm c} = 10$, $P_0 = 0.1 I_{2n_c}$, $\eta_0 = 0$, and $\tilde{\mathcal{H}} = H_1$. Figure 24(a) shows the time history of the performance z with the input nonlinearity present and z approaches zero in about 500 time steps. Figure 24(b) shows the input nonlinearity $\mathcal{N}$, Figure 24(c) and 24(d) show the auxiliary nonlinearity $\mathcal{N}_r$ and $\mathcal{N}_b$.

7. Hammerstein systems with arbitrary input nonlinearities

We now present numerical examples to illustrate the response of RCAC with auxiliary nonlinearities for the case where the input nonlinearities are neither odd nor even.

Example 7.1: We consider the asymptotically stable, minimum-phase plant,

$$G(\mathbf{z}) = \frac{1}{\mathbf{z} - 0.5} \tag{44}$$

with the input nonlinearity

$$\mathcal{N}(u) = \begin{cases} u^3, & \text{if } u < -1 \\ -u - 2, & \text{if } -1 \le u \le 1 \\ 3u^2 - 6, & \text{if } u > 1. \end{cases} \tag{45}$$

The command is $r(k) = \sin(0.2\pi k)$. Note that $d = 1$ and $H_d = 1$. As shown in Figure 25(a.i), the input nonlinearity $\mathcal{N}$ is one-to-one and onto and has the offset $\mathcal{N}(0) = -2$. Since $\mathcal{N}$ is non-monotonic and has partially overlapping intervals, and G is asymptotically stable, we choose $\mathcal{N}_{\rm sat}(u_c) = {\rm sat}_{p,q}(u_c)$, where $p = -10^6$ and $q = 10^6$ in Equation (20), let $\mathcal{N}_r(u_b) = -u_s$ for $u_s \in [-1, 1]$ and $\mathcal{N}_r(u_s) = u_s$ otherwise, and select $\mathcal{N}_s(u_b) = u_b$ so that the composite nonlinearity $\mathcal{N} \circ \mathcal{N}_r \circ \mathcal{N}_s$ is piecewise non-decreasing in Figure 25(a.ii). Knowledge of only the monotonicity of $\mathcal{N}$ is used to choose $\mathcal{N}_r$. To construct $\mathcal{N}_b$, note that piecewise non-decreasing input nonlinearity $\mathcal{N} \circ \mathcal{N}_r \circ \mathcal{N}_s$ has partially overlapping intervals. Therefore, we assume that $(\mathcal{N} \circ \mathcal{N}_r \circ \mathcal{N}_s)(1.29) = -1$ is known. We thus choose $\mathcal{N}_b(u_{\rm sat}) = 1$ for $u_{\rm sat} \in [-1, 1.29]$ and $\mathcal{N}_b(u_{\rm sat}) = u_{\rm sat}$ otherwise. Figure 25(a.iii) shows that the composite nonlinearity $\mathcal{N} \circ \mathcal{N}_r \circ \mathcal{N}_s \circ \mathcal{N}_b$ is non-decreasing. We let $n_c = 10$, $P_0 = 0.1 I_{2n_c}$, $\eta_0 = 0.1$, and $\tilde{\mathcal{H}} = H_1$. Figure 25(b) shows the resulting time history of z, while Figure 25(c) shows the time history of u. Finally, Figure 25(d) shows the frequency response of $G_{c,2000}(\mathbf{z})$, which indicates that $G_{c,2000}(\mathbf{z})$ has high gain at the command frequency 0.2π rad/sample.

Example 7.2: We consider the asymptotically stable, minimum-phase plant,

$$G(\mathbf{z}) = \frac{z - 0.3}{(z - 0.6)(z - 0.8)} \tag{46}$$

with the input nonlinearity (22). The command is $r(k) = \sin(0.2\pi k)$. Note that $d = 1$ and $H_d = 1$. As shown in Figure 26(a), the input nonlinearity $\mathcal{N}$ is neither one-to-one nor onto. Following the same procedures in Example 4.13, we thus choose $\mathcal{N}_b$, $\mathcal{N}_s$, and $\mathcal{N}_r$ as in Equations (23), (24), and (25), respectively. Figure 26(d) shows that the composite nonlinearity $\mathcal{N} \circ \mathcal{N}_r \circ \mathcal{N}_s \circ \mathcal{N}_b$ is non-decreasing. We let $n_{\rm c} = 10$, $P_0 = 0.01 I_{2n_c}$, $\eta_0 = 0.01$, and $\tilde{\mathcal{H}} = H_1$. Figure 26(e) shows the time history of the performance z with the input nonlinearity present and z approaches zero in about 1000 time steps and Figure 26(f) shows the time history of u. Figure 26(g) shows the input nonlinearity $\mathcal{N}$ and Figure 26(h) shows the time history of θ.

8. Conclusions

RCAC was applied to a command-following problem for Hammerstein systems. The input nonlinearities could be odd, even, or arbitrary, as well as monotonic or non-monotonic. RCAC was used with limited modelling information. In particular, RCAC uses knowledge of the first non-zero Markov parameter of the linear dynamics. To handle the effect of the non-monotonic nonlinearity, RCAC was augmented by auxiliary nonlinearities chosen based on the properties of the input nonlinearity. The auxiliary nonlinearities combine with the input nonlinearity to form a composite nonlinearity that is globally non-decreasing. Simulation results show that RCAC is able to follow the commands for the Hammerstein systems with an unknown disturbance when the composite input nonlinearity is globally non-decreasing.

Acknowledgements

We wish to thank Anthony D'Amato, Dogan Sumer, Jesse Hoagg, and Mohammad Al Janaideh for helpful discussions.

References

D'Amato, A.M., Sumer, E.D., & Bernstein, D.S. (2011a, December). *Frequency-domain stability analysis of retrospective-cost adaptive control for systems with unknown nonminimum-phase zeros*. Proceedings of IEEE Conference on Decision and Control (pp. 1098–1103). Orlando, FL.

D'Amato, A.M., Sumer, E.D., & Bernstein, D.S. (2011b, August). *Retrospective cost adaptive control for systems with unknown nonminimum-phase zeros (AIAA-2011-6203)*. Proceedings of AIAA Guidance, Navigation, and Control Conference. Portland, OR.

Fledderjohn, M.S., Holzel, M.S., Palanthandalam-Madapusi, H., Fuentes, R.J., & Bernstein, D.S. (2010, June). *A comparison of least squares algorithms for estimating Markov*

parameters. Proceedings of American Control Conference (pp. 3735–3740). Baltimore, MD.

Giri, F., & Bai, E.W. (2010). *Block-oriented nonlinear system identification*. London: Springer.

Haddad, W., & Chellaboina, V. (2001). Nonlinear control of Hammerstein systems with passive nonlinear dynamics. *IEEE Transactions on Automatic Control, 46*, 1630–1634.

Hoagg, J.B., & Bernstein, D.S. (2010, December). *Retrospective cost adaptive control for nonminimum-phase discrete-time systems. Part 1: The ideal controller and error system; Part 2: The adaptive controller and stability analysis*. Proceedings of IEEE Conference on Decision and Control (pp. 893–904). Atlanta, GA.

Hoagg, J.B., & Bernstein, D.S. (2011, June). *Retrospective cost model reference adaptive control for nonminimum-phase discrete-time systems. Part 1: The ideal controller and error system; Part 2: The adaptive controller and stability analysis*. Proceedings of American Control Conference (pp. 2927–2938). San Francisco, CA.

Hoagg, J.B., & Bernstein, D.S. (2012). Retrospective cost model reference adaptive control for nonminimum-phase systems. *AIAA Journal of Guidance, Control and Dynamics, 35*, 1767–1786.

Hoagg, J.B., Santillo, M.A., & Bernstein, D.S. (2008). Discrete-time adaptive command following and disturbance rejection for minimum phase systems with unknown exogenous dynamics. *IEEE Transactions on Automatic Control, 53*, 912–928.

Kung, M.C., & Womack, B.F. (1984a). Discrete-time adaptive control of linear dynamic systems with a two-segment piecewise-linear asymmetric nonlinearity. *IEEE Transactions on Automatic Control, 29*, 170–172.

Kung, M.C., & Womack, B.F. (1984b). Discrete-time adaptive control of linear systems with preload nonlinearity. *Automatica, 20*, 477–479.

Santillo, M.A., & Bernstein, D.S. (2010). Adaptive control based on retrospective cost optimization. *AIAA Journal of Guidance, Control, and Dynamics, 33*, 289–304.

Sumer, E.D., Holzel, M.H., D'Amato, A.M., & Bernstein, D.S. (2012). *FIR-based phase matching for robust retrospective-cost adaptive control*. Proceedings of American Control Conference (pp. 2707–2712). Montreal, Canada.

Tao, G., & Kokotović, P.V. (1996). *Adaptive control of systems with actuator and sensor nonlinearities*. New York: Wiley.

Venugopal, R., & Bernstein, D.S. (2000). Adaptive disturbance rejection using ARMARKOV system representations. *IEEE Transactions on Control Systems Technology, 8*, 257–269.

Yan, J., & Bernstein, D.S. (2013, June). *Adaptive control of uncertain Hammerstein systems with nonmonotonic input nonlinearities using auxiliary blocking nonlinearities*. Proceedings of American Control Conference (pp. 4915–4920). Washington, DC.

Yan, J., D'Amato, A.M., Sumer, E.D., Hoagg, J.B., & Bernstein, D.S. (2012, December). *Adaptive control of uncertain Hammerstein systems using auxiliary nonlinearities*. Proceedings of IEEE Conference on Decision and Control (pp. 4811–4816). Maui, HI.

Zaccarian, L., & Teel, A.R. (2011). *Modern anti-windup synthesis: Control augmentation for actuator saturation*. Princeton, NJ: Princeton University Press.